Title: Long-term Association between NO_2 and Human Mobility: A Two-year Spatiotemporal Study during the COVID-19 Pandemic in Southeast Asia

Authors: Zhaoyin Liu[1,2], Yangyang Li[2], Andrea Law[2], Jia Yu Karen Tan[2], Wee Han Chua[2], Yihan Zhu[3], Chen-Chieh Feng[2], Wei Luo[2,4] *

[1] School of Public Health, Nanjing Medical University, China, CN

[2] Department of Geography, National University of Singapore, Singapore, SG

[3] Department of Architecture, National University of Singapore, Singapore, SG

[4] Saw Swee Hock School of Public Health, National University of Singapore, Singapore, SG

*Corresponding author

Keywords: Spatio-Temporal Analysis, NO_2, Mobility, Southeast Asia**,** COVID-19

Abstract

Since the COVID-19 pandemic, governments have implemented lockdowns and movement restrictions to contain the disease outbreak. Previous studies have reported a significant positive correlation between NO_2 and mobility level during the lockdowns in early 2020. Though NO_2 level and mobility exhibited similar spatial distribution, our initial exploration indicated that the decreased mobility level did not always result in concurrent decreasing NO_2 level during a two-year time period in Southeast Asia with human movement data at a very high spatial resolution (i.e., Facebook origin-destination data). It indicated that factors other than mobility level contributed to NO_2 level decline. Our subsequent analysis used a trained Multi-Layer Perceptron model to assess mobility and other contributing factors (e.g., travel modes,

temperature, wind speed) and predicted future NO_2 levels in Southeast Asia. The model results suggest that, while as expected mobility has a strong impact on NO_2 level, a more accurate prediction requires considering different travel modes (i.e., driving and walking). Mobility shows two-sided impacts on NO_2 level: mobility above the average level has a high impact on NO_2, whereas mobility at a relatively low level shows negligible impact. The results also suggest that spatio-temporal heterogeneity and temperature also have impacts on NO_2 and they should be incorporated to facilitate a more comprehensive understanding of the association between NO_2 and mobility in the future study.

1 Introduction

With over 300 million confirmed cases and 5 million deaths, COVID-19 has spread all over the world since its inception (World Health Organization, 2022). To contain the COVID-19 outbreak, countries had imposed stringent lockdowns and restriction measures since 2020 (Lai *et al*., 2020; R. Zhu *et al*., 2022). Such public health control measures have caused an unintended positive consequence in terms of air quality improvement (Addas and Maghrabi, 2021; Faridi *et al.*, 2021).

Sharp declines in air pollution level have been observed during the lockdowns in early 2020 (Kanniah *et al.*, 2020; Kumar *et al.*, 2020; Tobías *et al.*, 2020; Zangari *et al.*, 2020; Addas and Maghrabi, 2021; Ghahremanloo *et al.*, 2021; Latif *et al.*, 2021; Calafiore *et al.*, 2022). Faridi *et al.* (2021) reported that the extent of air pollutant reduction may vary with the degree of lockdown measures. Wyche *et al.* (2021) inferred that the NO_2 decline during the UK lockdown period was due to the 70% vehicle traffic reduction. To investigate the correlation between the observed concurrent declines in NO_2 and mobility trend, some studies took advantages of the

mobility trend datasets (e.g., released by Google and Apple) in interpreting mobility level and demonstrated its significant positive correlation with NO_2 (Bao and Zhang, 2020; Li and Tartarini, 2020; Zhu *et al.*, 2020).

Although this large number of studies have observed NO_2 level decline and attributed the phenomenon to the reduction in mobility level, those studies focus more on the lockdowns in early 2020. Their investigations that were confined to a short time period for a few months did not account for other neglected factors which could also contribute to the observed pattern. Hence, the observed correlation between NO_2 and mobility was only limited to this short period and may not persist over a longer time period. Roberts-Semple *et al.*, (2021) reported that NO_2 exhibits seasonal characteristics in northeastern New Jersey. Zangari *et al.* (2020) found that the NO_2 level in New York City decreased between January and May in each year since 2015, with or without the lockdown in early 2020. In addition to temporal changes, mobility and NO_2 levels vary across regions and countries. By adopting the entire 2020 data in Singapore, Li *et al.* (2022) did confirm that it would not only overestimate the correlations between NO_2 and mobility if only focusing on the lockdown time period, but show significant spatial variations in the correlation between NO_2 and mobility as well. Thus, there is a demanding need to understand the spatio-temporal heterogeneity of NO_2 and mobility over a larger geographical area and a longer time period.

NO_2 is known to cause problems on environment and health (Tian *et al.*, 2019). Despite various mitigation measures implemented, such air pollutant has been a long-standing issue in Southeast Asia (SEA) (Kanniah *et al.*, 2020). During the COVID-19 pandemic, countries in SEA had imposed stringent lockdowns in 2020 along with various restriction measures (e.g., remote working, curfew, restrictions on

social gathering and traveling) which limited human movement and activities to a great extent (Luo *et al.*, 2022). These changes in human behaviours provided an unprecedented opportunity to study how decrease in citizens' mobility affects air pollution (Piccoli *et al.*, 2020). Thus, this study aims to perform spatio-temporal analyses of NO_2 level and mobility in SEA from March 2020 to February 2022 and develop a NO_2 prediction model to explore its response to key influencing factors. Different from previous studies, we utilized high-resolution mobility and NO_2 data in a two-year time period to investigate the long-term NO_2 response in SEA. The study aims to 1) identify the temporal changes of NO_2 and mobility throughout the two years of COVID-19 pandemic (March 2020 – February 2022); 2) evaluate the correlations between NO_2 and mobility; and 3) assess the impact of different factors on NO_2.

2 Materials and methods

2.1 Study area

Our study area consisted of 10 countries within SEA: Brunei, Cambodia, Indonesia, Laos, Malaysia, Myanmar, the Philippines, Singapore, Thailand, and Vietnam. We extracted and analysed NO_2 level, mobility, and other factors including travel modes, temperature, and haze from March 2020 to February 2022. This period was chosen because of reduced mobility due to government-mandated COVID-19 measures that occurred in different intensities and timescales across the countries, enabling direct comparison of mobility impact on NO_2 levels. The whole study area of 770 km^2 was square gridded to 0.25º for the follow-up analyses (Figure 1).

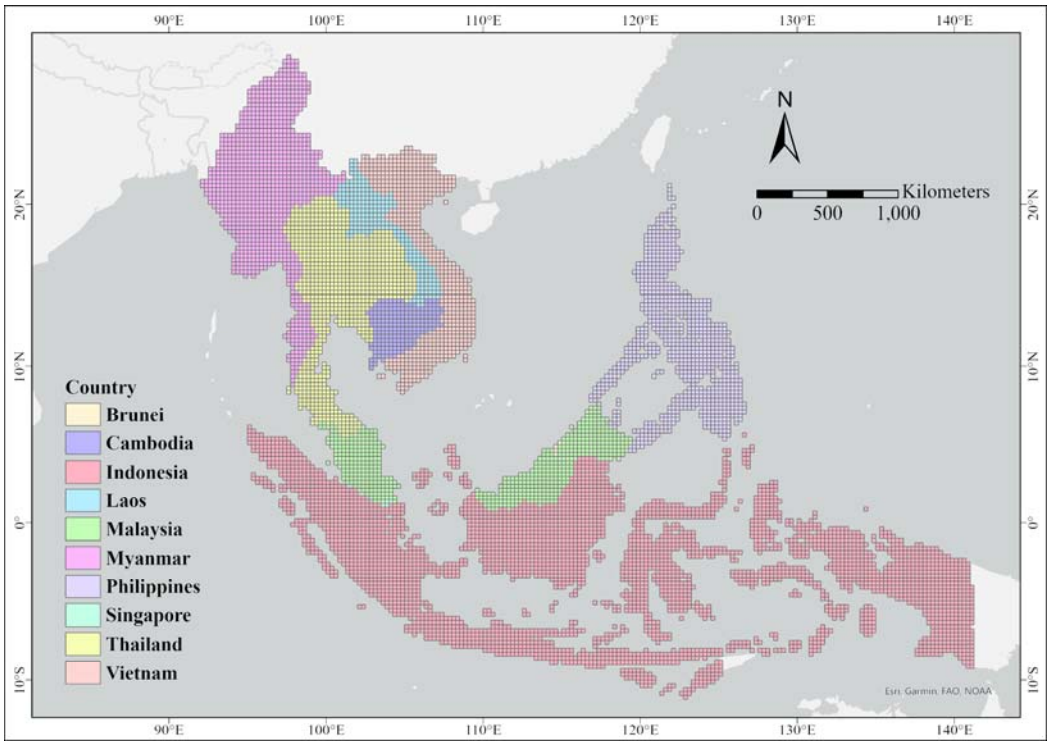

Figure 1. Area of study with coloured grids (0.25º × 0.25º) representing the different countries of interest within SEA.

2.2 Data sources and pre-processing

2.2.1 NO_2

The level-3 product of daily NO_2 observations (Tropospheric NO_2 column density) of TROPOMI/Sentinel-5 was obtained from the Google Earth Engine cloud-based platform. The original data was resampled from the source resolution of 0.01º to 0.25º through mean operator.

2.2.2 Mobility

This study adopted mobility data from Facebook Data for Good at Meta (Maas, 2019) and Apple Mobility Trends Reports (Apple, 2020). The Facebook movement dataset records user movements between origin and destination tiles aggregated using Facebook users' locations every eight hours (8:00, 16:00, 00:00). As the resolution of

Facebook's data in different countries varied from level 11 to level 14 (approximately 0.09° to 0.17°) in Bing tile system (Schwartz, 2018). We aggregated the original dataset to 0.25° grids by aggregating the mobility volumes within each grid (data records with 0m distance were excluded). As the dataset only contains information of the origin and destination rather than the actual movement route, it is difficult to assign movement value to other grids apart from the origin and destination grids, especially in long-distance travels. To minimize the inherent uncertainties in longer distance movements, the subsequent analyses are limited to movements whose origin and destination belong to the same or neighbouring grids (accounting for 93.33 percent of the total movement volume). The corresponding Facebook movement values were assigned equally to both starting and ending grids. Apple moving trends present the percentage changes of two travel modes, driving and walking over time. Note that, Apple moving trends data is calculated by referring to the number of searches carried out on its Maps application.

Meteorological conditions were reported to affect pollutant concentration (Pearce et al., 2011; He et al., 2016; Wang et al., 2017). We sourced six meteorological parameters that could potentially influence NO_2 level (Jiang et al., 2014; He et al., 2017) from 1st March 2020 to 31st December 2021: 1) maximum hourly 2m surface temperature, 2) dew point temperature, 3) mean hourly 10m u-component of wind, 4) 10m v-component of wind, 5) hourly precipitation, and 6) surface pressure. More specifically, we extracted each of these daily parameters from the ERA5 hourly reanalysis dataset from the Copernicus Climate Data Store (Copernicus, 2022) and aggregated them into daily meteorological values respectively.

2.2.3 Haze

Google Trends, an open-source database, was used to retrieve the indexed popularity of Google searches indicating the public's interest on that topic (Google, 2022). The English word 'haze' was used to understand the severity of haze at country level. We

utilised "pytrends" (an Application Programming Interface for Google Trends) to extract and scale datasets obtained for different countries, providing compatible datasets in both space and time (General Mills, 2022). While the values are indexed, which limits our ability to determine the actual number of searches, the set of varying values remains a useful proxy for the severity of haze in that location. Other keywords within and across the national languages were used in the search, but the results were noisy and excluded. For instance, searches for 'transboundary haze' were only detected in Singapore, Malaysia, and Indonesia, possibly denoting its prevalence only in those countries, or an issue of lexicons instead. Hence, only the English word 'haze' was employed as an approximation to the presence and severity of haze.

2.3 Data analyses

To address our study objectives, we incorporated three synergistic analyses: (1) a case study of Indonesia; (2) Space-Time Cube (STC) and Emerging Hotspot Analysis (EHSA) in SEA; (3) a Multi-Layer Perceptron (MLP) model to predict NO_2 and assess the impact of different input factors on NO_2. Due to the constraint of available data from Facebook movement dataset, we conducted the first two analyses with limited settings (Table 1). For the first analysis, we conducted a case study spanning a long time period to identify the temporal changes throughout the COVID-19 pandemic. Nevertheless, the complete dataset of 2020 is available only in Indonesia and Singapore. We chose to carry out our case study in Indonesia considering that it has a much larger spatial area than Singapore. The analysis expands to 10 countries in SEA from May 2021 because they are available for the whole of SEA. For the third analysis, our study covers a period between 1st April 2020 and 31st December 2021 because the meteorological data of 2022 was unavailable at the time this study was conducted.

166 *Table 1. An overview of the corresponding spatial extent, temporal resolution and*
167 *time period for each analysis.*

No	Analysis	Spatial extent	Temporal resolution	Time period
1	Case study of Indonesia	Indonesia	Monthly	March 2020 to February 2022
2	STC and EHSA	SEA	Weekly	31st May 2021 to 26th February 2022
3	MLP model	SEA	Daily	1st April 2020 to 31st December 2021

168

169 *2.3.1 Indonesia case study*

170 As the most populous country in SEA, the case study of Indonesia was conducted to
171 provide an initial and exploratory understanding of the linkage of mobility and NO_2
172 variations between March 2020 and February 2022. The monthly NO_2 data and
173 Facebook movement data in a spatial resolution of 0.25^{o} were studied across
174 Indonesia. Ordinary kriging (Wackernagel, 2003) was applied to fill in the grids
175 without data (Childs, 2004; Shad *et al.*, 2009). A series of continuous raster maps
176 were generated to facilitate the identification and subsequent interpretation of
177 potential patterns in Indonesia.

178

179 *2.3.2 Space-time hotspot analysis in SEA*

180 We used the EHSA tool in ArcGIS Pro 2.8 software (Esri, 2022) to detect
181 spatio-temporal trends in NO_2 and Facebook movement within their respective STC.
182 We conducted this analysis at a weekly interval between 31st May 2021 and 26th
183 February 2022 over the 10 countries in SEA. We then examined spatial clusters by

hot spot categories in greater detail through examining Pearson's correlation between the log of NO_2 level and the log of Facebook movement values over the 39-week period for each point in a spatial cluster. As the magnitude of the ranges of NO_2 (-5.10e-5 to 8.26e-4) and Facebook movement (2.50 to 8.28e+7) could potentially skew the analysis outcome, we performed data cleaning and transformation as below. Firstly, NO_2 data points with less than 1e-6 mol/m^2 and Facebook movement values below 50 were excluded as they were observed as noise (Figure 2). Then we conducted a logarithmic transformation of base 10 for both variables. Note that before taken logarithm, the filtered NO_2 data were multiplied by 10e+7 to ensure that data values remain positive. By removing data anomalies and reducing data skewness, these transformations improve the accuracy of our analyses.

Figure 2. Scatter plot between NO_2 and Facebook movement.

2.3.3 NO_2 prediction in SEA using MLP model

In addition to the correlation between NO_2 and mobility, we evaluated the impacts of different factors on NO_2 using an MLP model. MLP is the most popular feedforward model with good performance in air pollution prediction and forecasting (Cabaneros *et al.*, 2019; Shams *et al.*, 2021). It is an artificial neural network (ANN) that consists

of an input layer, an output layer, and multiple hidden layers in between. The number of nodes in the input layer should be the same as the number of input variables. Input variables included 15 parameters (Table 2) across five categories: location (i.e., longitude and latitude), elapsed days (i.e., the number of days since the start of the study period), meteorological parameters (i.e., rainfall, wind speed, u-component of wind, v-component of wind, temperature, dew-point temperature, surface pressure), haze, and mobility (i.e., Facebook movement, the logarithm of Facebook movement, Apple driving and walking trends). To improve the model performance of MLP, we adopted the same method for data transformation as mentioned in section 2.3.2.

Table 2. List of features in MLP model.

Feature category	**Feature meaning**	**Feature name**
Location	Longitude	lon
	Latitude	lat
Elapsed days	The number of days since the start of study period	day
Meteorological parameters	rainfall	rainfall
	wind speed	wind speed
	u-component of wind	u-wind
	v-component of wind	v-wind
	temperature	2m-temp
	dew-point temperature	dew-pt
	surface pressure	surface-p
Haze	relative number of haze searches	haze
Mobility	Facebook movement	facebook_movement
	logarithm of Facebook movement	log_facebook_movement
	Apple driving trend	apple_driving

	Apple walking trend	apple_walking

We used the rectified linear unit (ReLU) activation function in this MLP model. ReLU outputs negative values to 0 and keeps other values the same as the inputs. Therefore, we converted all the negative values to positive values using the transformation method as mentioned in 3.1.2. to improve the model efficiency. By training different MLP models, we could then determine the optimum model architecture to be used in this study that resulted in a smaller error with little additional computational effort. Of all the data records, 70% were used for training and while the remainder were used for testing. Each input variable was normalised before training the model. Root mean square error (RMSE), mean absolute error (MAE) and R^2 were used as the metrics for model evaluation.

We then used SHapley Additive exPlanation (SHAP) to explain the model in order to quantify the impact of the different features on the model output (Lundberg and Lee, 2017; Li, 2022). Traditional sensitivity analyses usually evaluate the changes in the output as a result of the change in only one input parameter. This may not be realistic as the possible correlation between variables is not accounted for. For example, air pressure and air temperature tend to increase or decrease together. SHAP values can account for the possible interactions amongst the input features when evaluating the impact of each feature on the output. However, it should be noted that the SHAP value or impact is different from the correlation. A high correlation means that the two variables tend to change together, while a higher SHAP value indicates a greater impact of one variable on the other, i.e., a change in one variable results in a greater magnitude of change in the other. The SHAP results can pinpoint the parameters that have relatively higher impacts on the NO_2 level in SEA.

3 Results & Discussion

3.1 Spatio-temporal distribution of NO_2 and mobility level in Indonesia

To begin with, we compared the spatio-temporal distribution variations of NO_2 and Facebook movement levels in Indonesia during March 2020 and February 2022. Overall, the result showed a decreasing trend during the study period except in March 2021 (Figure 3). On the other hand, NO_2 showed a cyclical trend in 2020 and an increasing trend in 2021 before reaching peak in October 2021.

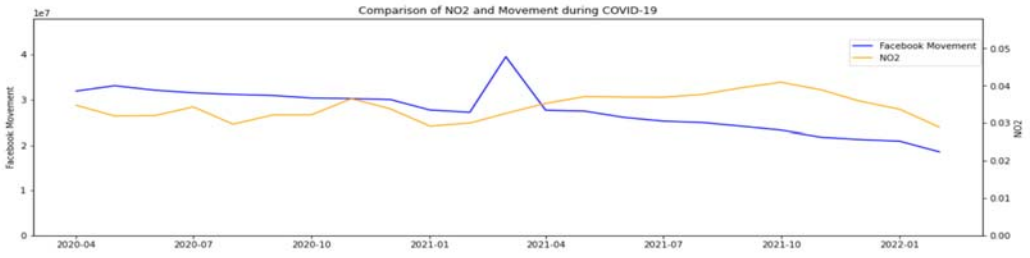

Figure 3. Comparison of Facebook movement and NO_2 in Indoensia.

South and West Indonesia showed high NO_2 levels, especially in Jakarta and its surrounding regions where the maximum mean NO_2 value reaches 1.01e-04 mol/m^2 in April 2020 (Figure 4). In comparison, the NO_2 level is substantially lower in other areas, especially in East Indonesia. Facebook movement presents a similar distribution. The similarity in distributions of Facebook movement and NO_2 level suggests a possible association between them.

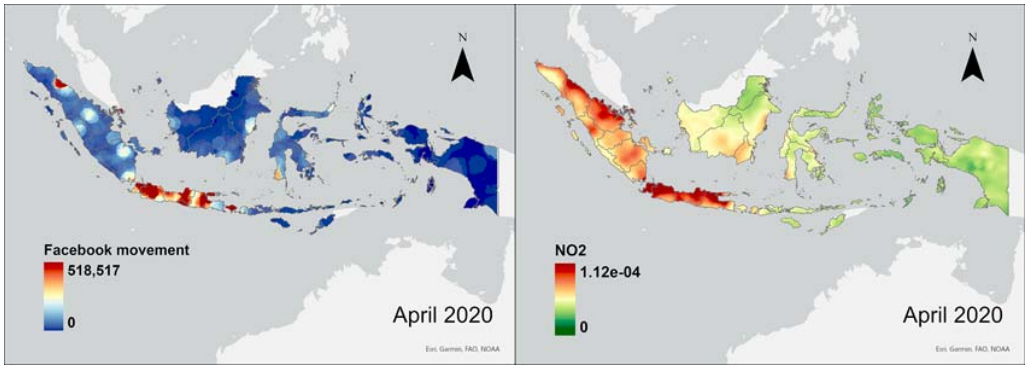

Figure 4. Spatial Distribution of Facebook movement and NO_2 level in April 2020.

Figures 5 and 6 illustrate the temporal changes in Facebook movement and NO_2 distribution. Maps showing the temporal variations over the last two years are presented in Appendix A. During the first wave of COVID-19, although Facebook movement did not vary significantly, NO_2 exhibited an oscillating pattern. Similarly, in 2021, the Facebook movement constantly decreased ever since March whereas the NO_2 level did not present a decreasing trend. Moreover, we observed an increase in NO_2 over the months in regions including Bali, Jawa Barat, Lampung and Kalimantan Barat. Overall, the temporal variation of NO_2 and Facebook movement did not present similarity. This result contradicts previous studies in which the reduction of mobility had led to a decrease in NO_2 level (Sicard *et al.*, 2020; Faridi *et al.*, 2021). Therefore, we hypothesise that human movement volume may not be the single significant factor affecting air pollution. For instance, forest fires had occurred in Indonesia causing air pollution and dryness which pre-matured the onset of haze in early 2021 (Hicks, 2021).

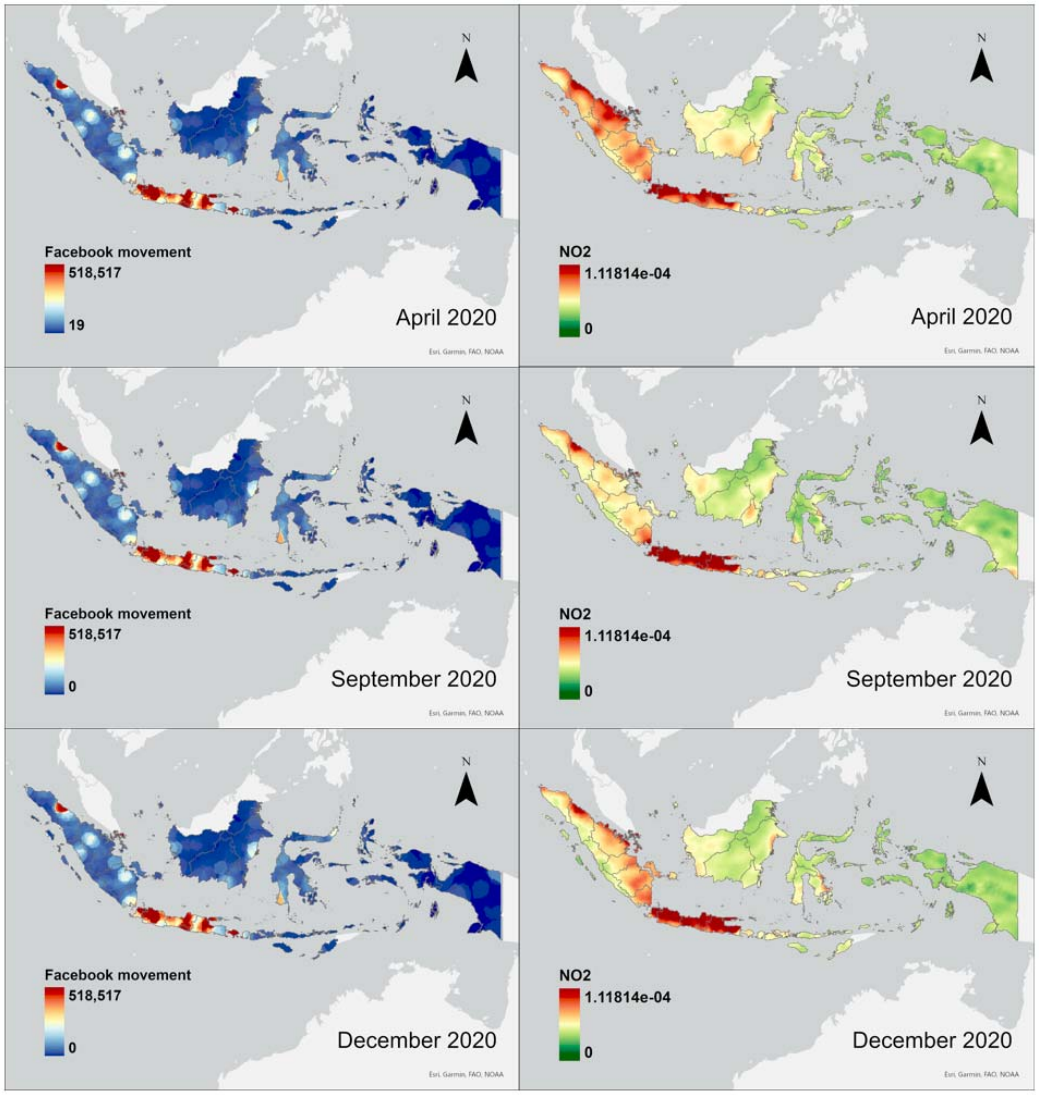

Figure 5. Comparison of Facebook movement and NO_2 level during the first wave (April 2020 – December 2020) of COVID-19 in Indonesia.

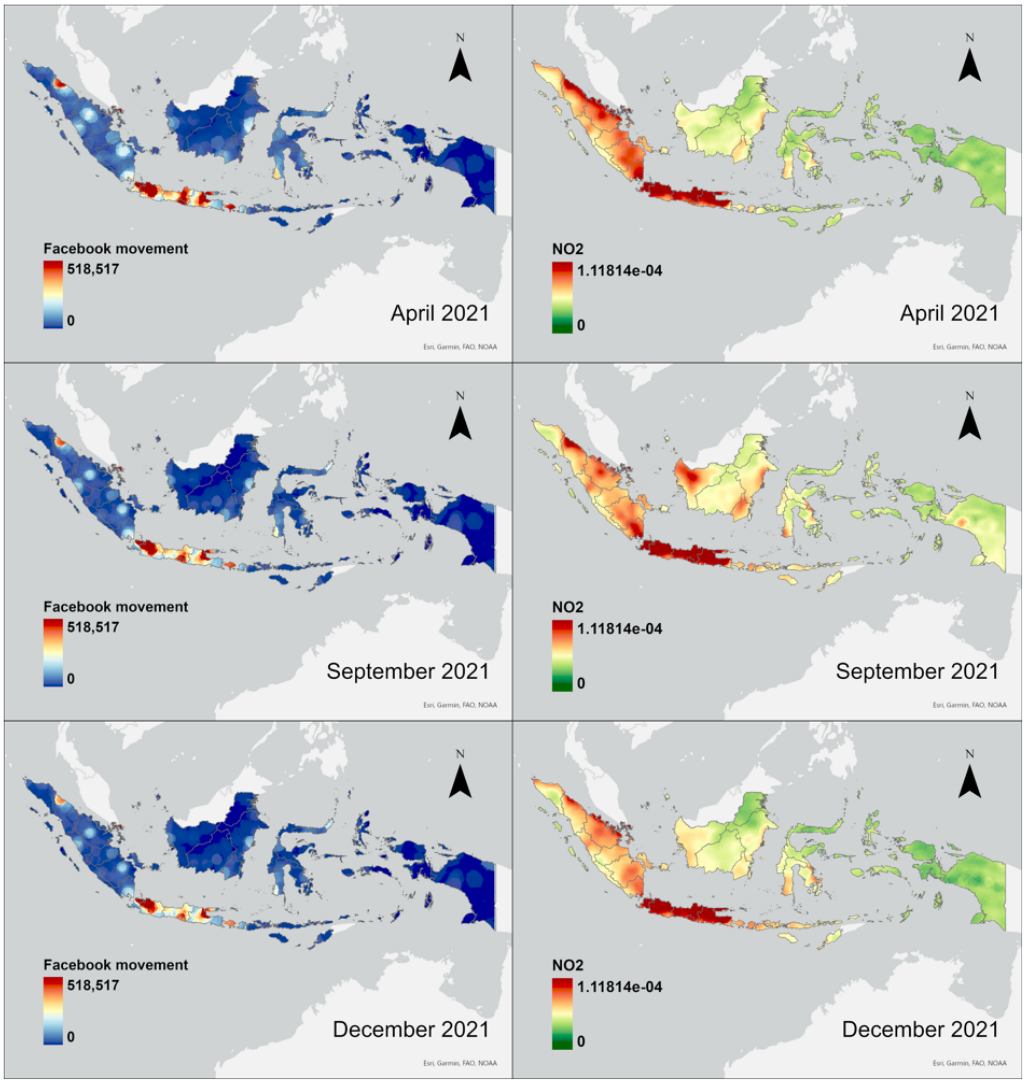

Figure 6. Comparison of Facebook movement and NO_2 level during the second wave of COVID-19 (April 2021 – December 2021) in Indonesia.

3.2 Spatio-temporal evaluation of the association between NO_2 and Facebook movement trends in SEA

Subsequently, we conducted analysis using EHSA at a finer temporal scale (weekly) in all selected SEA countries. Due to insufficient Facebook movement data, the study period for this analysis was limited to 31st May 2021 and 26th February 2022. Figure 7 shows the temporal changes in Log(NO_2) and Log(Facebook movement) during the study period. Similar to previous findings, there was a consistent pattern of a slight decrease in Facebook movement throughout the 39-week study period with a sharp decrease approximately at the 25th week in all eight SEA countries (Figure 7). On the other hand, we found no consistent patterns in NO_2 levels over time. Nonetheless, there was a slight increase in Log(NO_2) approximately around the 20th week and the 25th week in Thailand and Myanmar respectively.

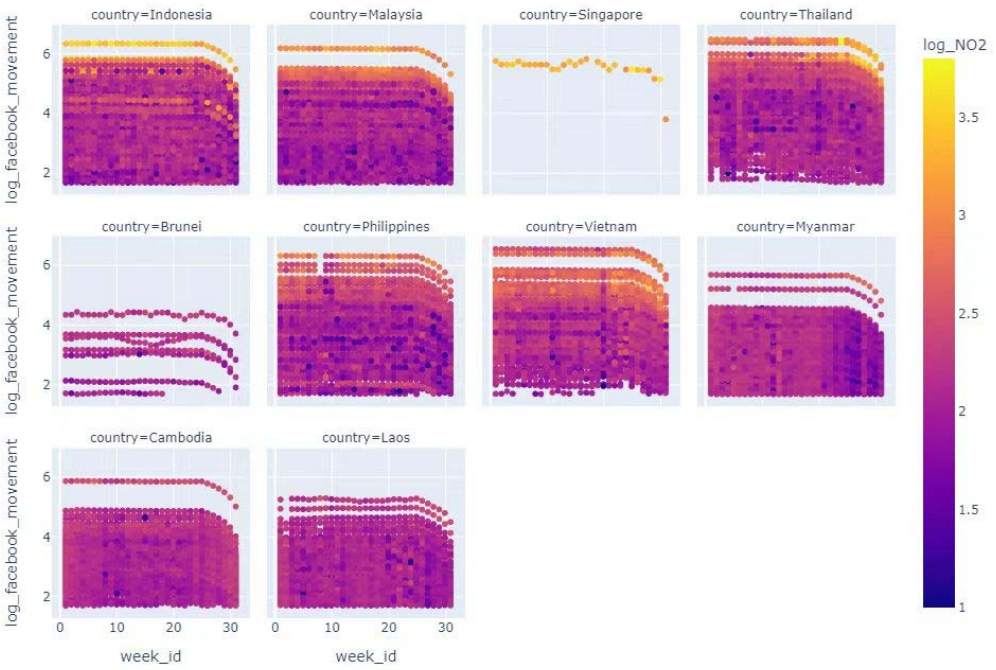

Figure 7. Change in Log(facebook_movement) against Log(NO_2) between June 2021 and February 2022. Each circle in the figure corresponds to a grid in the country. The darker the circle, the lower the Log(NO_2).

From the complete EHSA result derived from the NO_2 level (Figure 8a), it is observed that hot spots were detected mainly in the northwest of SEA. In comparison, central and south of SEA, which were mainly covered by Malaysia and Indonesia, were dominated by cold spots. Several hot spot patterns were identified, including new, intensifying, persistent and diminishing hot spots (Figure 8b). In terms of the spatial-temporal patterns of NO_2, the diminishing hot spots indicate decreasing clustering intensity of the NO_2 space-time hotspots in a statistically significant trend over time. Contrastingly, the intensifying hot spots showed a statistically significant increase in clustering intensity over time.

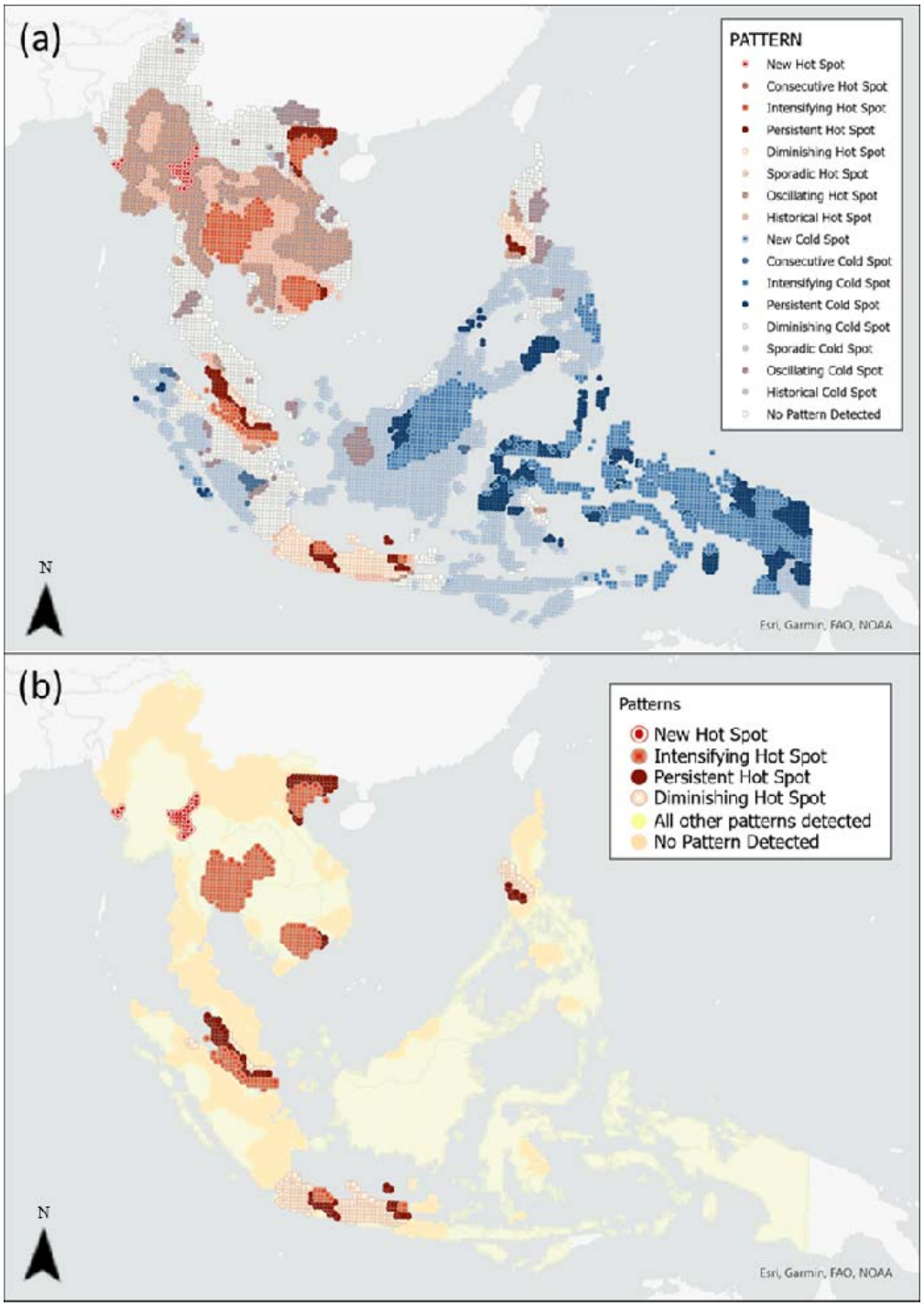

Figure 8. (a) Complete result of NO_2 EHSA result and (b) result of NO_2 EHSA with only selected patterns of interest.

The complete result of Facebook movement EHSA (Figure 9) is different from that of NO_2 EHSA (Figure 8a). The Facebook movement EHSA result showed substantially fewer observed patterns, where only diminishing, sporadic and historical hot spots but no cold spots were detected. In the context of Facebook movement, diminishing hot spots indicate that locations of statistically significant mobility hot spots exhibit decreasing clustering pattern. On the other hand, the sporadic hot spots indicate locations where statistically significant hot spots were only identified at some inconsistent time steps. Lastly, historical hot spots indicate locations where the level of mobility has been detected as statistically significant hot spots for the major time steps in the past. These hot spots are observed mostly in the major SEA cities such as Hanoi, Jakarta, Johor and Singapore, where lockdown restrictions would influence mobility more due to higher population and more intense economic activities (Heroy et al., 2021). This corroborates with the overall decrease in Facebook movement over the entire study period (Figure 7).

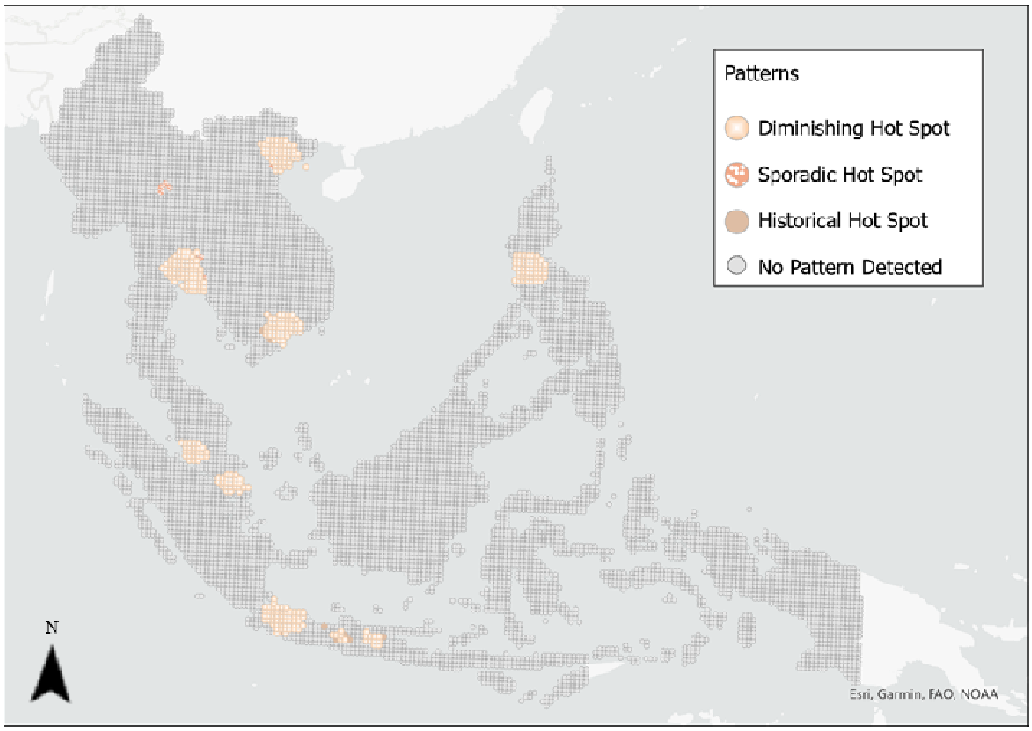

Figure 9. Complete EHSA result of Facebook movement.

As this study seeks to examine the effect of mobility changes on NO_2, we conducted correlation analyses on specific spatio-temporal patterns with reference to the EHSA results of NO_2. While several types of NO_2 spatio-temporal hot spots were identified using EHSA, the correlation between Log(NO_2) and Log(Facebook movement) varied widely geographically from June 2021 to February 2022. Such variation was observed within a country and even within a city.

In the case of the intensifying hot spots, while positive correlation between Log(NO_2) and Log(Facebook movement) was observed in Chon Buri province, Thailand, a mix of positive and negative correlations were observed in the Rayong and Chanthaburi provinces, Thailand (Figure 10). This trend did not support the previous findings that the degree of movement restriction correlates positively with NO_2 level. In fact, the same spatial cluster of NO_2 intensifying hot spots in Chon Buri and Rayong were identified as diminishing hot spots or no pattern detected in the Facebook movement EHSA result (Figure 9). While NO_2 levels at these locations became stronger hot spots over time, the corresponding mobility hot spots became less clustered. This contrasting observation further confirms that there is lack of evidence supporting a direct association between mobility and the resultant NO_2 levels.

344

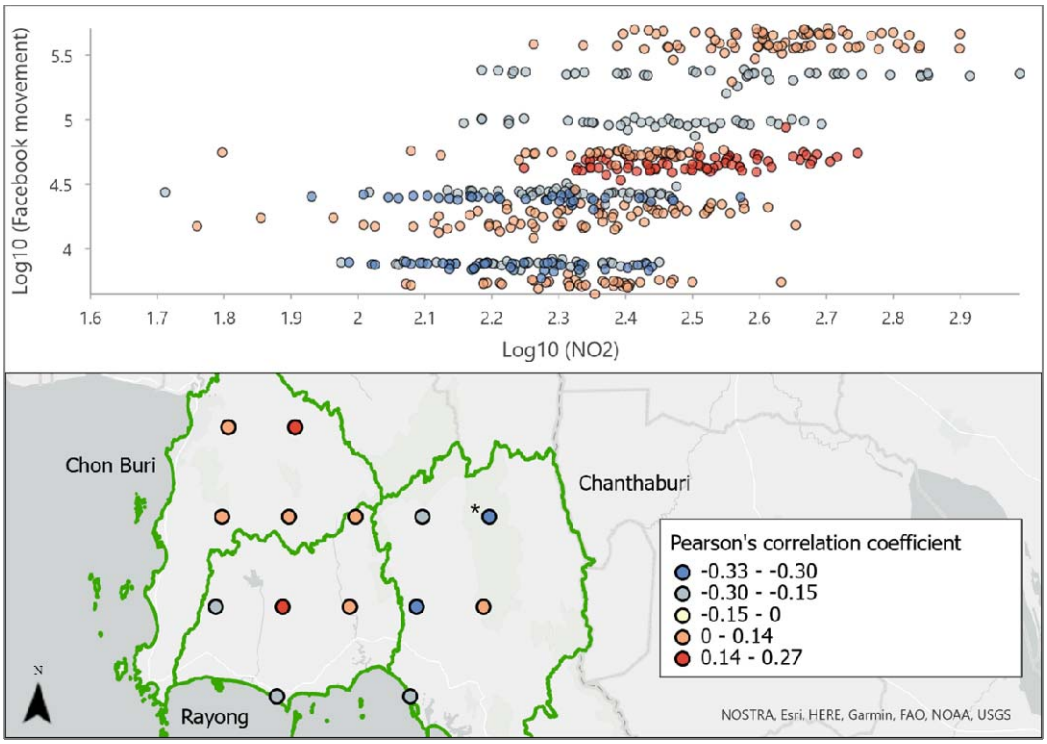

345

346 *Figure 10. Correlation between Log(Facebook movement) and Log(NO_2) in*
347 *intensifying hot spots in Thailand.*

348

349 Variation in correlation was also observed among the persistent hot spots in the
350 provinces around Ha Noi in Vietnam (Figure 11), and the new hot spots were found
351 along the border between Thailand and Myanmar (Figure 12). While the persistent hot
352 spots indicated statistically significant higher NO_2 levels relative to their space-time
353 neighbours over most of the 39 weeks without discernible trends, the new hot spots
354 indicate a statistically significant space-time hotspot only in the last time step and not
355 in any of the previous ones. Yet, the weak positive correlation and moderate negative
356 correlations between Log(NO_2) and Log(Facebook movement) show insubstantial
357 evidence to attribute the changes in NO_2 levels to the changes in mobility. Likewise,
358 these locations were identified as the diminishing hot spots or absence of space-time
359 pattern in the Facebook movement EHSA result (Figure 9). This similarly suggests

that while mobility hot spot intensity decreased in these points, the NO_2 hot spot intensity stayed relatively constant over time.

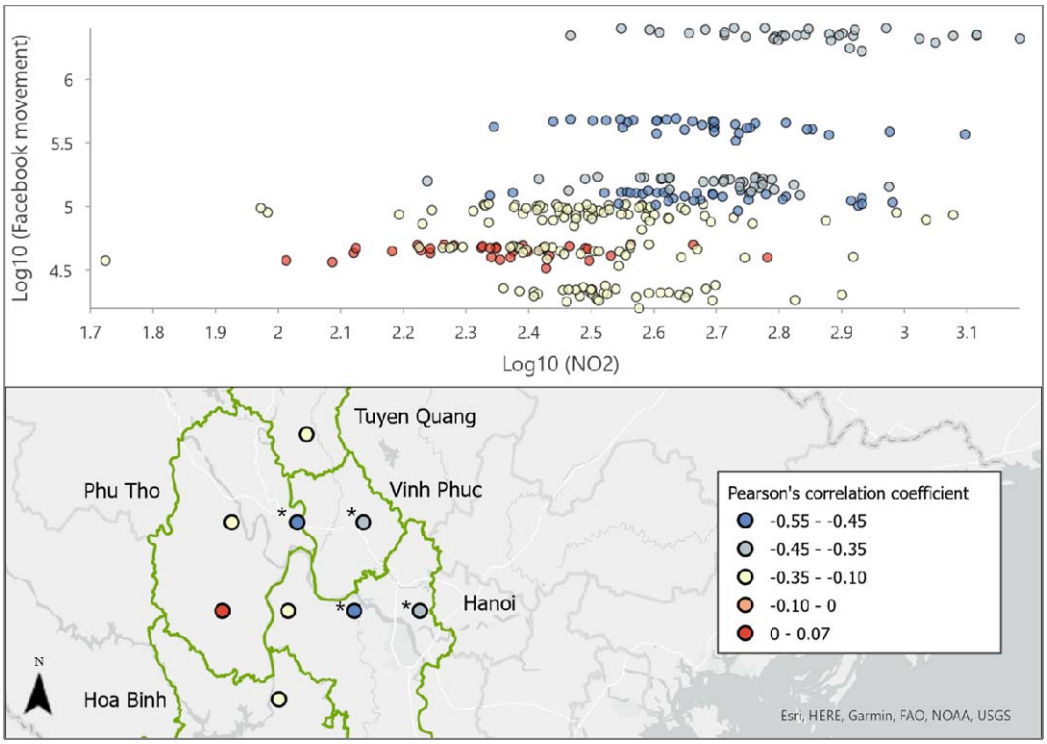

Figure 11. Correlation between Log(Facebook movement) and Log(NO_2) in persistent hot spots in Vietnam.

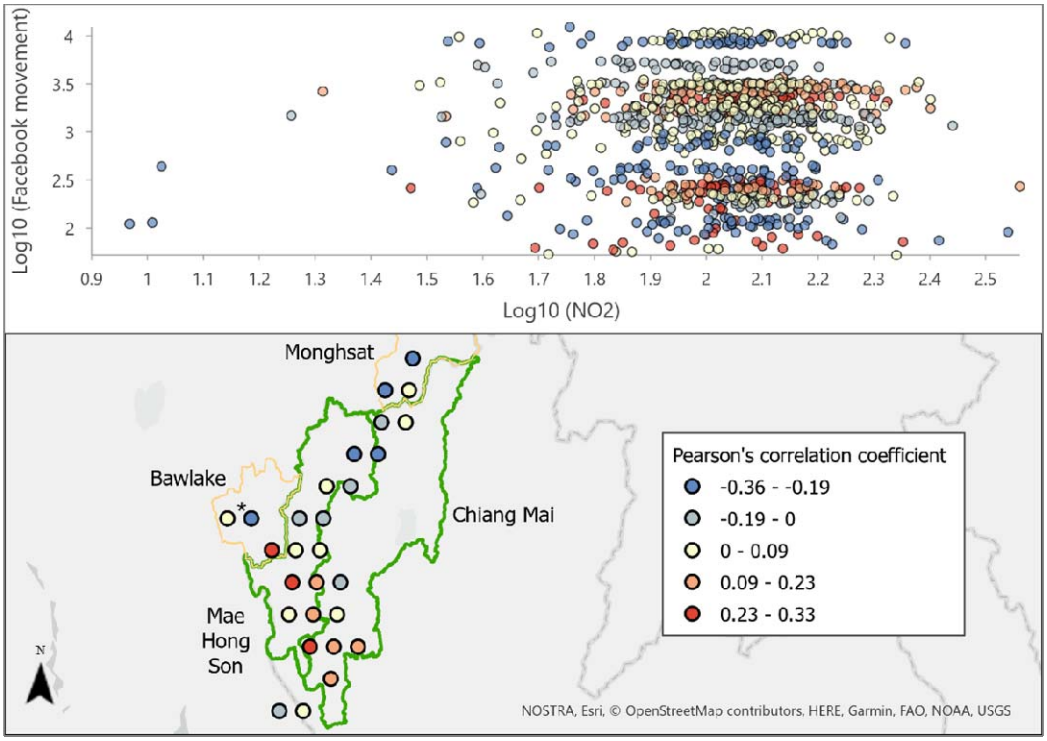

Figure 12. Correlation between log (Facebook movement) and log (NO_2) in new hot spots in Thailand and Myanmar.

In the case of the diminishing hot spots, we detected two clusters of points in Indonesia (Figure 13) and Malaysia (Figure 14), which exhibit positive correlations between Log(NO_2) and Log(Facebook movement). In addition, the corresponding points were also identified as the diminishing hot spots in the EHSA results of the Facebook movement. This suggests that both NO_2 levels and Facebook movement decrease over time, validating the positive correlation between these two variables.

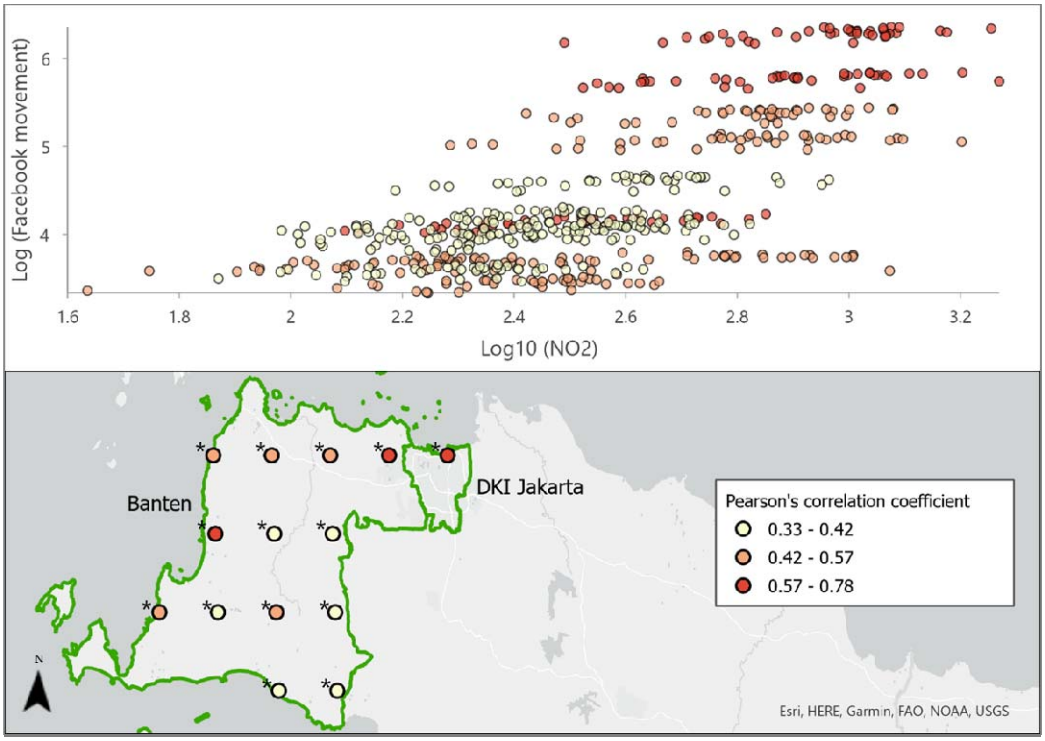

Figure 13. Correlation between Log(Facebook movement) and Log(NO_2) in diminishing hot spots Indonesia.

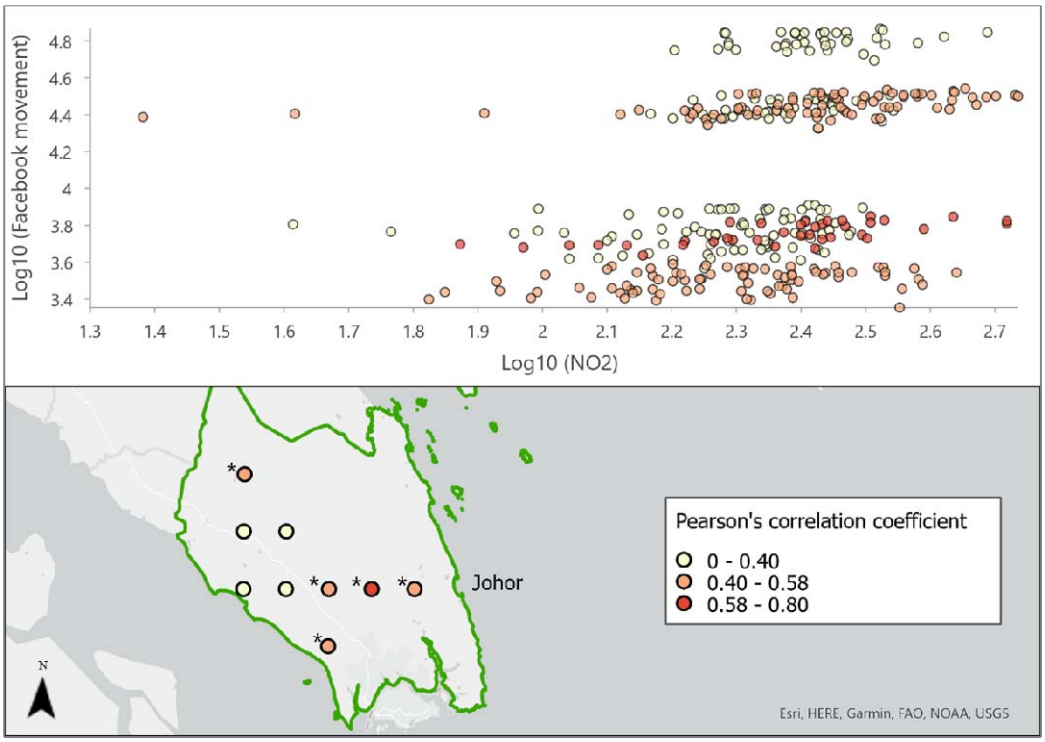

Figure 14. Correlation between Log(Facebook movement) and Log(NO_2) in diminishing hot spots in Malaysia.

Overall, these spatially explicit exploration of the correlation between NO_2 levels and mobility spatio-temporal trends revealed inconsistent patterns between June 2021 and February 2022, which approximates the period of the COVID-19 Delta and emerging Omicron variants. Further inspection of the correlation coefficients revealed that the observed correlations were only statistically significant for NO_2 diminishing hot spots and the negatively correlated NO_2 persistent and new hot spots. Therefore, we postulate that our SEA-wide EHSA results reinforce the findings from Li *et al.* (2022) where a national-scale spatial variability in correlations between NO_2 levels and mobility was observed. This strongly indicates that mobility alone could not fully explain the resultant NO_2 level changes over time and space.

3.3 NO_2 prediction and its sensitivity to different influential factors

The previous two sections suggest that mobility is not the single influencing factor on the NO_2 variation over time. We further explored the association between NO_2 and other potential factors using the MLP model. Firstly, the correlation coefficients between each pair of variables were calculated and plotted as a heatmap (Figure 15). Log(facebook_movement) is the variable that has the strongest correlation with both Log(NO_2) and NO_2 (i.e., the correlation coefficient of 0.45 and 0.42, respectively). In comparison, Apple driving and walking trends have a much weaker correlation with Log(NO_2) (i.e., the correlation coefficient of -0.13 and -0.02, respectively). However, Apple driving trend is strongly correlated to Apple walking trend, with a correlation coefficient of 0.73. This shows that Apple driving and Apple walking trends are very likely to increase or decrease together. Apart from the three mobility factors, longitude, latitude and temperature also showed a relatively strong correlation with NO_2 and Log(NO_2).

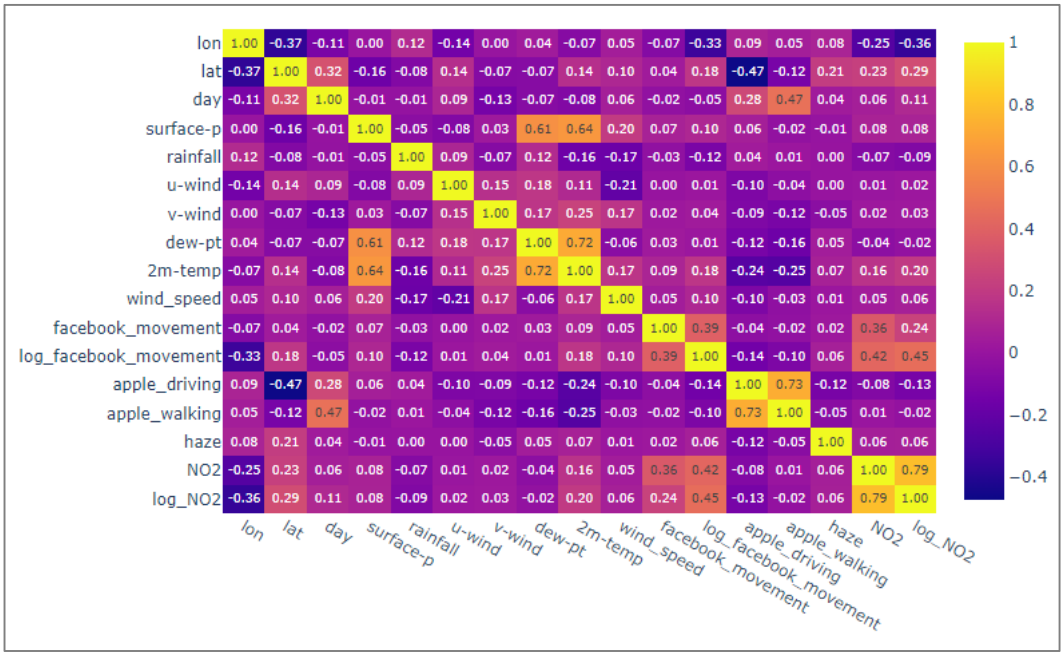

Figure 15. Correlation matrix between any pair of variables.

After calculating the coefficients, 15 features (Table 2) were used to predict the output NO_2 in the MLP model. The model architecture consists of 18 hidden layers with a range of 8 to 64 nodes in each layer, and a total of 14,793 trainable parameters. Figure 16 plots the predicted and the measured ground-truth output values in both the training and testing datasets. A higher difference was observed at low Log(NO_2) levels. Table 3 summarized the performance of both the training and testing datasets where the high similarity between their respective RMSE and MAE values suggests that no overfitting was found.

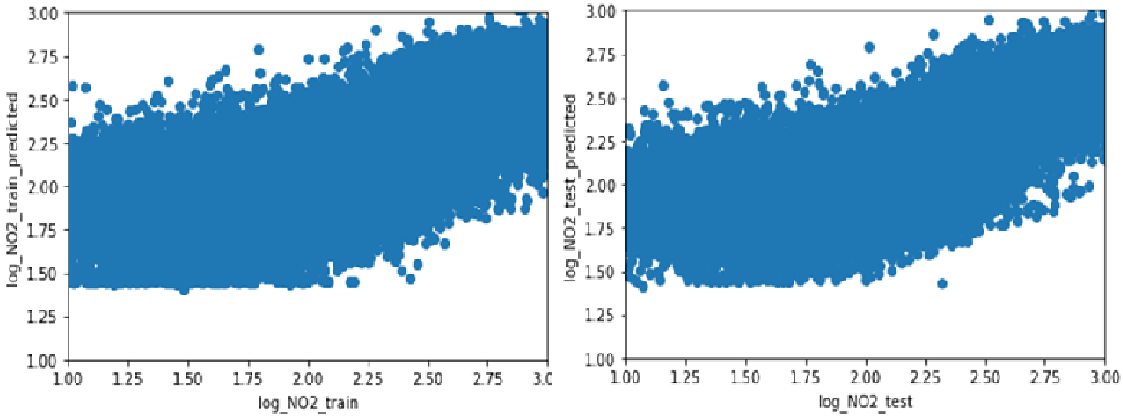

Figure 16. The predicted and measured Log(NO_2) in the training (left) and testing (right) dataset.

Table 3. Performance of the MLP model on training and testing dataset.

	RMSE (NO_2; mol/m^2)	**RMSE (Log(NO_2))**	**MAE (NO_2; mol/m^2)**	**MAE (Log(NO_2))**	**R^2 (NO_2)**	**R^2 (Log(NO_2))**
Train	1.03e-05	0.22	5.03e-06	0.16	0.49	0.52
Test	1.02e-05	0.22	5.02e-06	0.16	0.49	0.52

The prediction error was evaluated by calculating the difference between the predicted and measured ground truth values in the testing dataset. The histogram of prediction error shows that most errors fall between -0.5 and 0.5 (Figure 17). A

coloured distinction was used to differentiate observations with large prediction errors (> 0.5 or < -0.5) from those with small prediction errors (Figure 18). This distinction revealed that large errors concentrate at column densities lower than 1e-5.5 mol/m^2 (or log(NO_2) < 1.5). A measured NO_2 column density of 1e-5.5 mol/m^2 could be overestimated as 1e-5 mol/m^2. On the other hand, measurements also have uncertainty. By comparing with ground measurements, the uncertainty in measurement was about 1e-5 mol/m^2 (Tonion & Pirotti, 2022). While our prediction error occurred mostly at small NO_2 column densities and was within the range of measurement uncertainty, this implies that the trained model performs well in predicting most of the NO_2 levels and can generalise such prediction without overfitting the models.

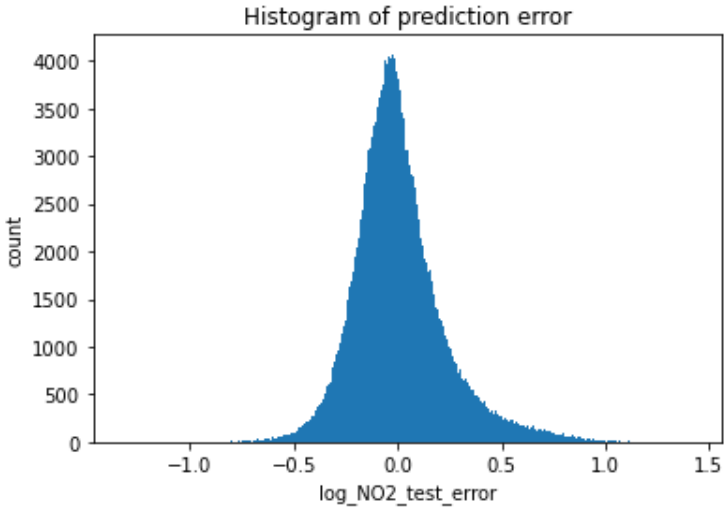

Figure 17. Histogram of prediction errors in the testing dataset.

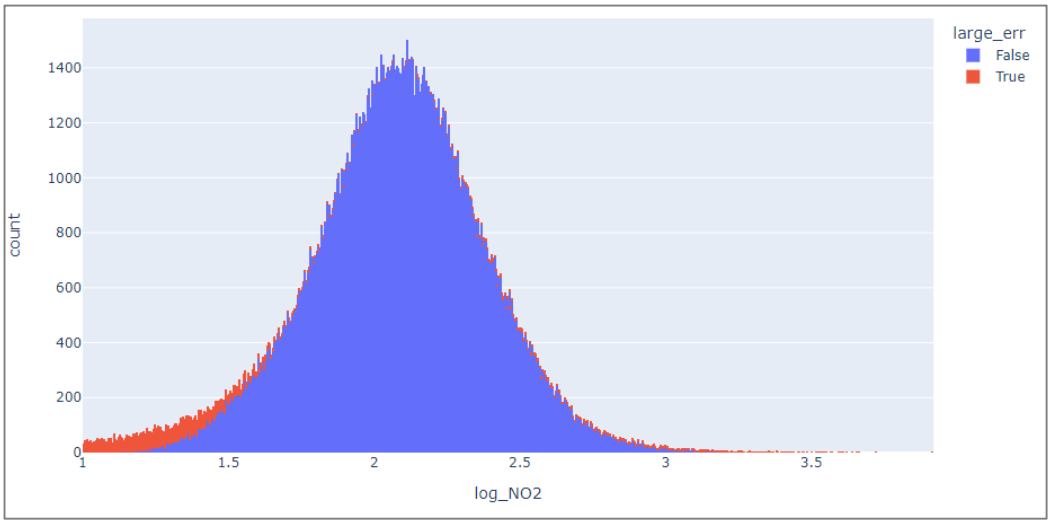

Figure 18. The distribution of large errors in the measured Log(NO_2) in the testing dataset.

Subsequently, data records with high Log(NO_2) were sliced as a new dataset to investigate its association with different parameters. This included 6362 Log(NO_2) records ranging between 2.48 to 2.50 with small prediction error, representing a subset of data reliably predicted by the model. SHAP values were calculated for each parameter in each record representing the magnitude of impact each parameter has on the output Log(NO_2).

The spatial (i.e., lat and lon) and temporal information (i.e., day) had the highest impacts on the output Log(NO_2) according to the global interpretation summary (Figure 19). This reinforces the importance of spatial and temporal information in predicting NO_2 levels. Besides spatial and temporal parameters, the next highest contributing parameters were mobility factors (i.e., apple_walking, apple_driving and facebook_movement). Specifically, the Apple moving trends had higher impacts on NO_2 as compared to the Facebook movement. As mentioned, Facebook movement data has higher spatial resolution than Apple's. Although the latter is coarser in

resolution, it distinguished different travel modes (i.e., driving and walking). The comparatively higher impacts of Apple moving trends on Log(NO_2) suggest that distinguishing different travel modes is important in predicting NO_2. Additionally, other factors especially temperature also showed impacts to a certain extent on this model, although their impact is overall lower compared to spatio-temporal factors and most of the mobility factors.

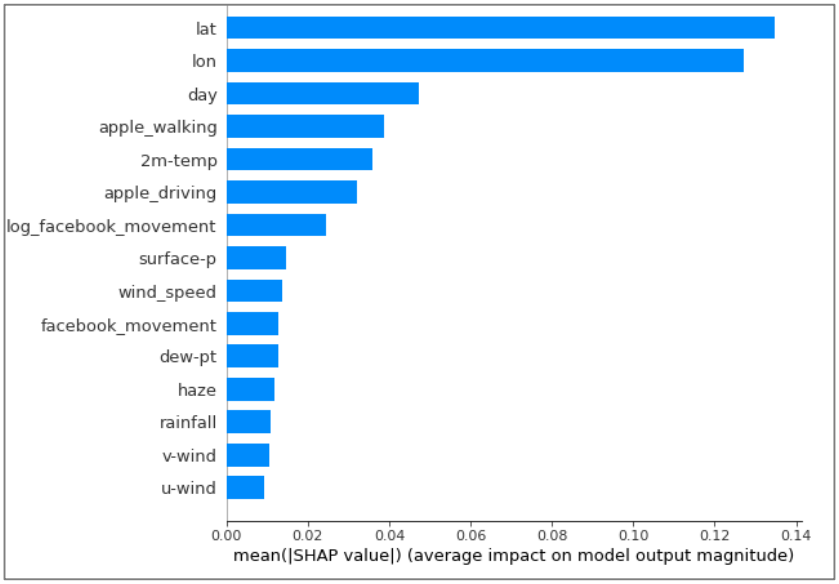

Figure 19. A summary plot of impacts of each parameter on Log(NO_2).

The dependence plot in Figure 20 shows that when Log(facebook_movement) is below the average value (normalised to 0), both facebook movement and apple moving trend hardly have any impact on NO_2. In other words, the impact of change in mobility parameters on NO_2 is more detectable at higher movement level. On the other hand, this impact on NO_2 could be different at the same total movement level. For instance, when Log(facebook_movement) was above the mean value, the blue points (lower level of Apple driving trend) have lower SHAP values compared to the pink points (higher level of Apple driving trend). This suggests that when total mobility is contributed less by the driving trend, an increase in total mobility could be contributed more by the walking trend instead. Therefore, there tends to be a lower resultant impact on NO_2 levels.

In addition, the impact of Apple walking trend on Log(NO_2) in Figure 21 shows that there is a negative impact on Log(NO_2) when the walking trend decreases. The different interactions of Apple driving and Apple walking indicated that this negative impact on Log(NO_2) from a decreased walking trend could be attributed to the concurrent decrease in Apple driving trend (in blue colour).

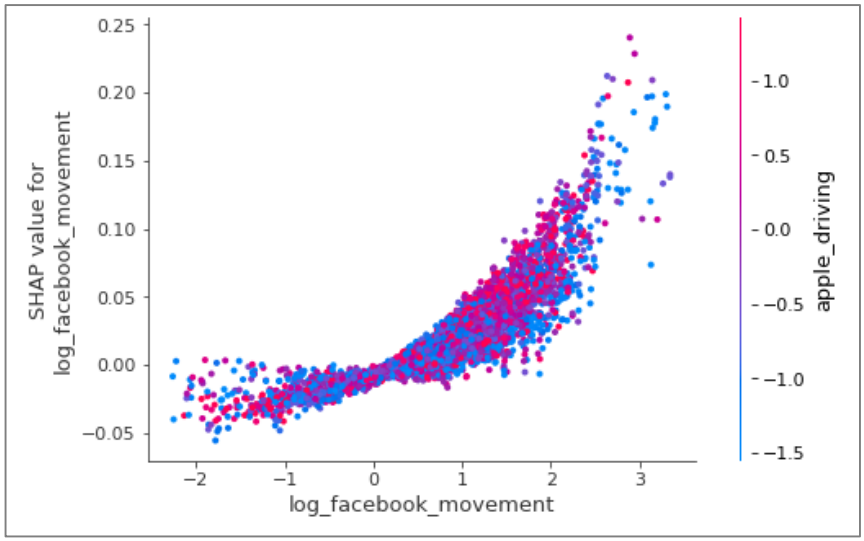

Figure 20. Impact of Log(facebook_movement) on Log(NO_2) represented by the SHAP values at different Log(facebook_movement) values along the x-axis, and its interactions with Apple driving trend (in colour).

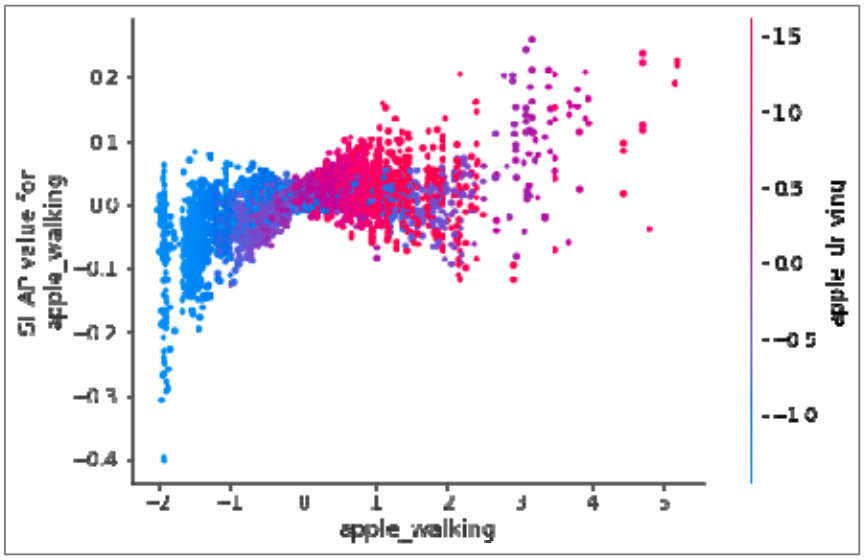

Figure 21. Impact of Apple walking trend on Log(NO_2) represented by the SHAP values at different apple_walking values along the x-axis, and its interactions with Apple driving trend (in colour).

4 Conclusions

The various lockdowns and movement restrictions during the COVID-19 pandemic present an opportunity to study how air pollution varies along with the decrease of mobility. Although existing studies have conducted analysis during the lockdowns in early 2020 and observed a positive correlation between NO_2 and mobility. Given that their study period was confined to a short time period, their observation may be subject to other under-examined factors. Therefore, we investigated the variability of NO_2 at a very large spatial scale with diverse human movement patterns in a two-year study time period. We found that mobility showed decreasing trend during the COVID-19 pandemic in Indonesia. However, the decreased mobility did not generally result in concurrent decrease in NO_2 during the two years. Our EHSA results revealed the spatio-temporal heterogeneity in NO_2 levels and mobility in SEA during June 2021 and February 2022. The variability in Pearson's correlation coefficient further indicated the absence of a definitive correlation between NO_2 and Facebook

507 movement. The subsequent MLP result suggests that mobility with distinguished
508 travel modes substantially influenced the MLP model and NO_2 prediction. Moreover,
509 the impact of mobility on NO_2 varies with mobility level. When mobility is below the
510 average level, its impact on NO_2 becomes negligible. This may be another reason why
511 the decrease in mobility did not result in any expected correlated decrease in NO_2 in
512 general.

513

514 Our findings denoted that the reduced mobility during COVID-19 pandemic did
515 contribute to the variation of NO_2. Nevertheless, other meteorological factors
516 especially temperature also had considerable impacts and should be considered along
517 with mobility when attempting to understand NO_2 variation. Although SEA countries
518 are gradually loosening movement and other restrictions to restore industry activities
519 and economy (Luo *et al.*, 2022), traffic control is still a recommended solution for
520 regions suffering from poor air quality. Additionally, our model provides an accurate
521 NO_2 prediction method, which could be adopted as a health risk warning system in
522 preventing possible exposure to high concentration of NO_2.

523

524 There are three main limitations in this study and further investigations are
525 recommended. Firstly, our study mainly estimated the movement value in adjacent
526 study grids, excluding long distance travels. Although daily commuting in adjacent
527 grids accounts for most of the movement value (93.33 percent), this would cause
528 some uncertainty in actual movement volume estimation. Future studies could adopt
529 other datasets that include specific mobility trajectories to account for long distance
530 travel patterns and reduce uncertainty. Secondly, as this study seeks to examine the
531 spatio-temporal changes in NO_2 levels, only specific patterns of hot spots (i.e., new,
532 intensifying, persistent and diminishing hot spot) were selected for correlation

533 analyses. Other studies could examine the correlation between NO_2 and mobility
534 levels for other patterns of hot spots and even the cold spots to potentially elicit more
535 insights. Finally, this study did not adopt a spatio-temporal machine learning model
536 due to the discontinuous Facebook movement data (i.e., most countries have missing
537 data before May 2021) during the two-year study period. Future studies are
538 recommended to adopt a hybrid model (e.g., convolutional neural network (CNN) and
539 long short-term memory (LSTM)) for NO_2 prediction. Nonetheless, it presented
540 timely and novel evidence that the spatial and temporal information were strong
541 factors in explaining NO_2 levels. Future scholars are recommended to adopt a hybrid
542 model (e.g., convolutional neural network (CNN) and long short-term memory
543 (LSTM)) in NO_2 prediction to account for the interactions of NO_2 with time and
544 space.

545

546 Source codes related to this study can be found on a public GitHub repository
547 (https://github.com/liyangyang515/Spatio-Temporal-Patterns-of-NO_2-and-Mobility-T
548 hrough-the-Variants-of-COVID-19-in-SEA).

549

550 **Acknowledgements**

551 The Facebook Movement between Tiles data are not publicly available, the
552 permission of usage was granted by Facebook Data for Good Partner Program.

553

554 **References**

555 Addas, A., & Maghrabi, A. (2021). The Impact of COVID-19 Lockdowns on Air
556 Quality—A Global Review. Sustainability, 13(18), 10212.
557 https://doi.org/10.3390/su131810212

558 Apple. (2020). COVID□19 Mobility Trends Reports. Retrieved from
559 https://www.apple.com/covid19/mobility. Accessed April 7, 2022

560 Archer, C., Cervone, G., Golbazi, M., Al Fahel, N. & Hultquist, C. (2020). Changes
561 in air quality and human mobility in the USA during the COVID-19 pandemic.
562 Bulletin of Atmospheric Science and Technology, 1(3), pp.491-514.
563 https://doi-org/10.1007/s42865-020-00019-0

564 Bao, R., & Zhang, A. (2020). Does lockdown reduce air pollution? Evidence from 44
565 cities in northern China. Science of The Total Environment, 731, 139052.
566 https://doi.org/10.1016/j.scitotenv.2020.139052

567 Bekkar, A., Hssina, B., Douzi, S. & Douzi, K. (2021), Air-pollution prediction in
568 smart city, deep learning approach, Journal of Big Data, vol. 8, no. 1.
569 https://doi.org/10.1186/s40537-021-00548-1

570 Cabaneros, S.M., Calautit, J.K. and Hughes, B.R., 2019. A review of artificial neural
571 network models for ambient air pollution prediction. Environmental
572 Modelling & Software, 119, pp.285-304.
573 https://doi.org/10.1016/j.envsoft.2019.06.014

574 Cahyadi, M.N., Handayani, H.H., Warmadewanthi, I., Rokhmana, C.A., Sulistiawan,
575 S.S., Waloedjo, C.S., Raharjo, A.B., Endroyono, Atok, M., Navisa, S.C.,
576 Wulansari, M. & Jin, S. (2022). Spatiotemporal Analysis for COVID-19 Delta
577 Variant Using GIS-Based Air Parameter and Spatial Modeling, International

578 Journal of Environmental Research and Public Health, vol. 19, no. 3, p. 1614.
579 https://doi.org/10.3390/ijerph19031614

580 Calafiore, A., Macdonald, J. L., & Singleton, A. (2022). Decomposing the Temporal
581 Signature of Nitrogen Dioxide Declines during the COVID-19 Pandemic in
582 UK Urban Areas. Applied Spatial Analysis and Policy.
583 https://doi.org/10.1007/s12061-022-09438-2

584 Casquero-Vera, J.A., Lyamani, H., Titos, G., Borrás, E., Olmo, F.J. &
585 Alados-Arboledas, L. (2019). Impact of primary NO2 emissions at different
586 urban sites exceeding the European NO2 standard limit, Science of The Total
587 Environment, 646, 1117–1125. https://doi.org/10.1016/j.scitotenv.2018.07.360

588 Castelli, M., Clemente, F.M., Popovič, A., Silva, S. & Vanneschi, L. (2020). A
589 Machine Learning Approach to Predict Air Quality in California, Complexity,
590 vol. 2020, pp. 1–23. https://doi.org/10.1155/2020/8049504

591 Cenek, M., Haro, R., Sayers, B., & Peng, J. (2018). Climate change and power
592 security: Power load prediction for rural electrical microgrids using long short
593 term memory and artificial neural networks. Applied Sciences, 8(5), 749.
594 https://doi.org/10.3390/app8050749

595 Chen, L.-W.A., Chien, L.-C., Li, Y. & Lin, G. (2020). Nonuniform impacts of
596 COVID-19 lockdown on air quality over the United States, Science of The
597 Total Environment, 745, 141105.
598 https://doi.org/10.1016/j.scitotenv.2020.141105

599 Childs, C. (2004). Interpolating surfaces in ArcGIS spatial analyst. ArcUser,
600 July-September, 3235(569), 32–35.

601 Copernicus. (2022). Climate Data Store. Retrieved from
602 https://cds.climate.copernicus.eu/. Accessed August 30, 2022,

603 Esri. (2022). Emerging Hot Spot Analysis (Space Time Pattern Mining). Retrieved
604 from
605 https://pro.arcgis.com/en/pro-app/2.8/tool-reference/space-time-pattern-minin
606 g/emerginghotspots.htm. Accessed April 30, 2022

607 European Environmental Agency. (2019). Emissions of the main air pollutants by
608 sector group in the EEA-33. Retrieved from:
609 https://www.eea.europa.eu/data-and-maps/daviz/share-of-eea-33-emissions-4.
610 Accessed April 23, 2022

611 Faridi, S., Yousefian, F., Janjani, H., Niazi, S., Azimi, F., Naddafi, K., & Hassanvand,
612 M. S. (2021). The effect of COVID-19 pandemic on human mobility and
613 ambient air quality around the world: A systematic review. Urban Climate, 38,
614 100888. https://doi.org/10.1016/j.uclim.2021.100888

615 General Mills. (2014). Retrieved from: https://github.com/GeneralMills/pytrends.
616 Accessed August 30, 2022

617 Ghahremanloo, M., Lops, Y., Choi, Y., & Mousavinezhad, S. (2021). Impact of the
618 COVID-19 outbreak on air pollution levels in East Asia. Science of The Total
619 Environment, 754, 142226. https://doi.org/10.1016/j.scitotenv.2020.142226

620 Google. (2022). Google Trends. Retrieved from https://trends.google.com/. Accessed
621 April 30, 2022

622 Hale, T., Angrist, N., Goldszmidt, R., Kira, B., Petherick, A., Phillips, T., Webster, S.,
623 Cameron-Blake, E., Hallas, L., Majumdar, S. & Tatlow, H. (2021). A global
624 panel database of pandemic policies (Oxford COVID-19 Government
625 Response Tracker). Nature Human Behaviour, vol. 5, pp. 1–10.
626 https://doi.org/10.1038/s41562-021-01079-8

627 Hassoun, Y., James, C. & Bernstein, D.I. (2019). The Effects of Air Pollution on the
628 Development of Atopic Disease. Clinical Reviews in Allergy & Immunology,
629 57, 403–414. https://doi-org/10.1007/s12016-019-08730-3

630 Heroy, S., Loaiza, I., Pentland, A. & O'Clery, N. (2021). COVID-19 policy analysis:
631 labour structure dictates lockdown mobility behaviour. Journal of The Royal
632 Society Interface, Royal Society, 18, 20201035.
633 https://doi.org/10.1098/rsif.2020.1035

634 He, J., Gong, S., Yu, Y., Yu, L., Wu, L., Mao, H., Song, C., Zhao, S., Liu, H., Li, X.,
635 & Li, R. (2017). Air pollution characteristics and their relation to
636 meteorological conditions during 2014–2015 in major Chinese cities.
637 Environmental Pollution, 223, 484–496.
638 https://doi.org/10.1016/j.envpol.2017.01.050

639 He, J., Yu, Y., Xie, Y., Mao, H., Wu, L., Liu, N., & Zhao, S. (2016). Numerical
640 Model-Based Artificial Neural Network Model and Its Application for
641 Quantifying Impact Factors of Urban Air Quality. Water, Air, & Soil Pollution,
642 227(7), 235. https://doi.org/10.1007/s11270-016-2930-z

643 Hicks, R. (2021). The haze is likely to hit Southeast Asia early in 2021 - is climate
644 change to blame?. Eco-Business. Retrieved from:
645 https://www.eco-business.com/news/the-haze-is-likely-to-hit-southeast-asia-ea
646 rly-in-2021-is-climate-change-to-blame/. Accessed April 20, 2022.

647 Jiang, N., Dirks, K. N., & Luo, K. (2014). Effects of local, synoptic and large-scale
648 climate conditions on daily nitrogen dioxide concentrations in Auckland, New
649 Zealand. International Journal of Climatology, 34(6), 1883–1897.
650 https://doi.org/10.1002/joc.3808

651 Kanniah, K. D., Kamarul Zaman, N. A. F., Kaskaoutis, D. G., & Latif, M. T. (2020).
652 COVID-19's impact on the atmospheric environment in the Southeast Asia
653 region. Science of The Total Environment, 736, 139658.
654 https://doi.org/10.1016/j.scitotenv.2020.139658

655 Kumar, P., Hama, S., Omidvarborna, H., Sharma, A., Sahani, J., Abhijith, K. V.,
656 Debele, S. E., Zavala-Reyes, J. C., Barwise, Y., & Tiwari, A. (2020).
657 Temporary reduction in fine particulate matter due to 'anthropogenic
658 emissions switch-off' during COVID-19 lockdown in Indian cities.
659 Sustainable Cities and Society, 62, 102382.
660 https://doi.org/10.1016/j.scs.2020.102382

661 Lai, S., Ruktanonchai, N. W., Zhou, L., Prosper, O., Luo, W., Floyd, J. R.,
662 Wesolowski, A., Santillana, M., Zhang, C., Du, X., Yu, H., & Tatem, A. J.
663 (2020). Effect of non-pharmaceutical interventions to contain COVID-19 in
664 China. Nature, 585(7825), 410–413.
665 https://doi.org/10.1038/s41586-020-2293-x

666 Latif, M. T., Dominick, D., Hawari, N. S. S. L., Mohtar, A. A. A., & Othman, M.
667 (2021). The concentration of major air pollutants during the movement control
668 order due to the COVID-19 pandemic in the Klang Valley, Malaysia.
669 Sustainable Cities and Society, 66, 102660.
670 https://doi.org/10.1016/j.scs.2020.102660

671 Latza, U., Gerdes, S. & Baur, X. (2009). Effects of nitrogen dioxide on human health:
672 Systematic review of experimental and epidemiological studies conducted
673 between 2002 and 2006. International Journal of Hygiene and Environmental
674 Health, 212, 271–287. https://doi.org/10.1016/j.ijheh.2008.06.003

675 Li, J. and Tartarini, F., (2020). Changes in Air Quality during the COVID-19
676 Lockdown in Singapore and Associations with Human Mobility Trends.

677 Aerosol and Air Quality Research, 20(8), pp.1748-1758.
678 https://doi.org/10.4209/aaqr.2020.06.0303

679 Li, Y., Zhu, Y., Tan, J.Y.K., Teo, H.C., Law, A., Qu, D. and Luo, W., (2022). The
680 impact of COVID-19 on NO_2 and PM2. 5 levels and their associations with
681 human mobility patterns in Singapore. Annals of GIS, pp.1-17.
682 https://doi.org/10.1080/19475683.2022.2121855

683 Li, Z. (2022). Extracting spatial effects from machine learning model using local
684 interpretation method: An example of SHAP and XGBoost. Computers,
685 Environment and Urban Systems, 96, 101845.
686 https://doi.org/10.1016/j.compenvurbsys.2022.101845

687 Liu, F., Wang, M. & Zheng, M. (2021). Effects of COVID-19 lockdown on global air
688 quality and health. Science of The Total Environment, vol. 755, p. 142533.
689 https://doi.org/10.1016/j.scitotenv.2020.142533

690 Lundberg, S. M., & Lee, S. I. (2017). A unified approach to interpreting model
691 predictions. Advances in neural information processing
692 systems, pp. 4765-4774

693 Luo, W., Liu, Z., Zhou, Y., Zhao, Y., Li, Y. E., Masrur, A., & Yu, M. (2022).
694 Investigating Linkages Between Spatiotemporal Patterns of the COVID-19
695 Delta Variant and Public Health Interventions in Southeast Asia: Prospective
696 Space-Time Scan Statistical Analysis Method. JMIR Public Health and
697 Surveillance, 8(8), e35840. https://doi.org/10.2196/35840

698 Ma, Y., Zhao, Y., Liu, J., He, X., Wang, B., Fu, S., Yan, J., Niu, J., Zhou, J., Luo, B.,
699 (2020). Effects of temperature variation and humidity on the death of
700 COVID-19 in Wuhan, China. Science of Total Environment. 724, 138226.
701 https://doi.org/10.1016/j.scitotenv.2020.138226

Maas, P. (2019). Facebook Disaster Maps: Aggregate Insights for Crisis Response & Recovery. The 25th ACM SIGKDD Conference on Knowledge Discovery and Data Mining, 3173–3173.

Mo, C., D. Tan, T. Mai, C. Bei, J. Qin, W. Pang, and Z. Zhang. (2020). An Analysis of Spatiotemporal Pattern for COIVD-19 in China Based on Space-time Cube. Journal of Medical Virology 92: 1587–1595. https://doi-org/10.1002/jmv.25834

Nakada, L.Y.K. & Urban, R.C. (2020). COVID-19 pandemic: Impacts on the air quality during the partial lockdown in São Paulo state, Brazil. Science of The Total Environment, 730, 139087.

Nyhan, M.M., Kloog, I., Britter, R., Ratti, C. & Koutrakis, P. (2018), Quantifying population exposure to air pollution using individual mobility patterns inferred from mobile phone data. Journal of Exposure Science & Environmental Epidemiology, vol. 29, no. 2, pp. 238–247. https://doi.org/10.1038/s41370-018-0038-9

Rahman, N.H.A., Lee, M.H., Suhartono, & Latif, M.T. (2016). Evaluation performance of time series approach for forecasting air pollution index in Johor, Malaysia. Sains Malays 45(11): 1625-1633.

Pan, X., Zhao, Y. & Wang, M. (2021). Impact of COVID-19 on Extremely Polluted Air Quality and Trend Forecast in Seven Provinces and Three Cities of China. Frontiers in Environmental Science, vol. 9. https://doi.org/10.3389/fenvs.2021.7709

Park, Y.M. & Kwan, M.-P. (2017). Individual exposure estimates may be erroneous when spatiotemporal variability of air pollution and human mobility are

ignored. Health & Place, vol. 43, pp. 85–94. https://doi.org/10.1016/j.healthplace.2016.10.002

Pearce, J. L., Beringer, J., Nicholls, N., Hyndman, R. J., Uotila, P., & Tapper, N. J. (2011). Investigating the influence of synoptic-scale meteorology on air quality using self-organizing maps and generalized additive modelling. Atmospheric Environment, 45(1), 128–136. https://doi.org/10.1016/j.atmosenv.2010.09.032

Piccoli, A., Agresti, V., Balzarini, A., Bedogni, M., Bonanno, R., Collino, E., Colzi, F., Lacavalla, M., Lanzani, G., Pirovano, G., Riva, F., Riva, G.M. & Toppetti, A.M. (2020). Modeling the Effect of COVID-19 Lockdown on Mobility and NO2 Concentration in the Lombardy Region, Atmosphere, Multidisciplinary Digital Publishing Institute, 11, 1319. https://doi.org/10.3390/atmos11121319

Purwanto, P., Utaya, S., Handoyo, B., Bachri, S., Astuti, I.S., Utomo, K.S.B. & Aldianto, Y.E. (2021). Spatiotemporal Analysis of COVID-19 Spread with Emerging Hotspot Analysis and Space–Time Cube Models in East Java, Indonesia. ISPRS International Journal of Geo-Information, vol. 10, no. 3, p. 133. https://doi.org/10.3390/ijgi10030133

Qin, D., Yu, J., Zou, G., Yong, R., Zhao, Q. & Zhang, B. (2019) A Novel Combined Prediction Scheme Based on CNN and LSTM for Urban PM2.5 Concentration. IEEE Access, vol. 7, pp. 20050–20059. https://doi.org/10.1109/ACCESS.2019.2897028

Roberts-Semple, D., Song, F. & Gao, Y. (2012) Seasonal characteristics of ambient nitrogen oxides and ground–level ozone in metropolitan northeastern New Jersey. Atmospheric Pollution Research, 3, pp. 247–257. https://doi.org/10.5094/APR.2012.027

751 Roy, S., Saha, M., Dhar, B., Pandit, S. & Nasrin, R. (2020), Geospatial analysis of
752 COVID-19 lockdown effects on air quality in the South and Southeast Asian
753 region, Science of The Total Environment, p. 144009.
754 https://doi.org/10.1016/j.scitotenv.2020.144009

755 Ritchie, H., Mathieu, E., Rodés-Guirao, L., Appel, C., Giattino, C., Ortiz-Ospina, E.,
756 Hasell, J., Macdonald, B., Beltekian, D., and Roser, M. (2020). Coronavirus
757 Pandemic (COVID-19). Retrieved from
758 https://ourworldindata.org/coronavirus. Accessed April 20, 2022

759 Saadat, S., Rawtani, D., Hussain, C.M. (2020). Environmental perspective of
760 COVID-19. Science of Total Environment. 728, pp.138870.
761 https://doi.org/10.1016/j.scitotenv.2020.138870.

762 Schwartz, J. (2018). Bing Maps Tile System. Retrieved from
763 https://docs.microsoft.com/en-us/bingmaps/articles/bing-maps-tile-system.
764 Accessed April 20, 2022

765 Shad, R., Mesgari, M. S., abkar, A., & Shad, A. (2009). Predicting air pollution using
766 fuzzy genetic linear membership kriging in GIS. Computers, Environment and
767 Urban Systems, 33(6), 472–481.
768 https://doi.org/10.1016/j.compenvurbsys.2009.10.004

769 Shams, S.R., Jahani, A., Kalantary, S., Moeinaddini, M. and Khorasani, N., (2021).
770 Artificial intelligence accuracy assessment in NO_2 concentration forecasting
771 of metropolises air. Scientific Reports, 11(1), pp.1-9. https://doi.org
772 /10.1038/s41598-021-81455-6

773 Shapley, L.S., (1953). Quota solutions op n-person games1. Edited by Emil Artin and
774 Marston Morse, pp.343.

775 Sicard, P., De Marco, A., Agathokleous, E., Feng, Z., Xu, X., Paoletti, E., Rodriguez,
776 J.J.D. & Calatayud, V. (2020). Amplified ozone pollution in cities during the
777 COVID-19 lockdown. Science of The Total Environment, 735, 139542.
778 https://doi.org/10.1016/j.scitotenv.2020.139542

779 Syetiawan, A., Harimurti, M., & Prihanto, Y., (2022). A spatiotemporal analysis of
780 COVID-19 transmission in Jakarta, Indonesia for pandemic decision support,
781 Geospatial Health, vol. 17, no. S1. https://doi.org/10.4081/gh.2022.1042

782 Tunlathorntham, S., & Thepanondh, S. (2017). Prediction of Ambient Nitrogen
783 Dioxide Concentrations in the Vicinity of Industrial Complex Area, Thailand.
784 Air, Soil and Water Research, vol. 10, p. 117862211770090.
785 https://doi.org/10.1177/1178622117700906

786 Tadano, Y.S., Potgieter-Vermaak, S., Kachba, Y.R., Chiroli, D.M.G., Casacio, L.,
787 Santos-Silva, J.C., Moreira, C.A.B., Machado, V., Alves, T.A., Siqueira, H. &
788 Godoi, R.H.M. (2021). Dynamic model to predict the association between air
789 quality, COVID-19 cases, and level of lockdown, Environmental Pollution,
790 vol. 268, no. Pt B, p. 115920. https://doi.org/10.1016/j.envpol.2020.115920

791 Tian, Y., Yao, X. & Chen, L. (2019). Analysis of spatial and seasonal distributions of
792 air pollutants by incorporating urban morphological characteristics,
793 Computers, Environment and Urban Systems, 75, 35–48.
794 https://doi.org/10.1016/j.compenvurbsys.2019.01.003

795 Tiwari, A., Gupta, R., & Chandra, R. (2021). Delhi air quality prediction using LSTM
796 deep learning models with a focus on COVID-19 lockdown. ArXiv,
797 abs/2102.10551. https://doi.org/10.48550/arXiv.2102.10551

798 Tobías, A., Carnerero, C., Reche, C., Massagué, J., Via, M., Minguillón, M. C.,
799 Alastuey, A., & Querol, X. (2020). Changes in air quality during the lockdown

in Barcelona (Spain) one month into the SARS-CoV-2 epidemic. Science of The Total Environment, 726, 138540. https://doi.org/10.1016/j.scitotenv.2020.138540

Tonion, F. and Pirotti, F. (2022). SENTINEL-5P NO2 DATA: CROSS-VALIDATION AND COMPARISON WITH GROUND MEASUREMENTS. The International Archives of Photogrammetry, Remote Sensing and Spatial Information Sciences, 43, pp.749-756.

Wackernagel, H. (2003). Ordinary kriging. Multivariate Geostatistics, Springer, Berlin, Heidelberg. pp. 79-88.

Wang, A., Xu, J., Tu, R., Saleh, M. & Hatzopoulou, M. (2020). Potential of machine learning for prediction of traffic related air pollution. Transportation Research Part D: Transport and Environment, vol. 88, p. 102599. https://doi.org/10.1016/j.trd.2020.102599

Wang, Y., Fu, X., Jiang, W., Wang, T., Tsou, M.-H., & Ye, X. (2017). Inferring urban air quality based on social media. Computers, Environment and Urban Systems, 66, 110–116. https://doi.org/10.1016/j.compenvurbsys.2017.07.002

World Health Organization 2022, WHO Coronavirus (COVID-19) Dashboard. Retrieved from covid19.who.int. Accessed March 10, 2022.

Wihayati & Wibowo, F.W. (2021). Prediction of air quality in Jakarta during the COVID-19 outbreak using long short-term memory machine learning. IOP Conference Series: Earth and Environmental Science, vol. 704, no. 1, p. 012046.

Wu, Y. & Song, G. (2019). The Impact of Activity-Based Mobility Pattern on Assessing Fine-Grained Traffic-Induced Air Pollution Exposure. International

824 Journal of Environmental Research and Public Health, vol. 16, no. 18, p. 3291.
825 https://doi.org/10.3390/ijerph16183291

826 Wu, C., He, H., Song, R. & Peng, Z. (2022). Prediction of air pollutants on roadside
827 of the elevated roads with combination of pollutants periodicity and deep
828 learning method, Building and Environment, vol. 207, p. 108436.
829 https://doi.org/10.1016/j.buildenv.2021.108436

830 Wyche, K. P., Nichols, M., Parfitt, H., Beckett, P., Gregg, D. J., Smallbone, K. L., &
831 Monks, P. S. (2021). Changes in ambient air quality and atmospheric
832 composition and reactivity in the South East of the UK as a result of the
833 COVID-19 lockdown. Science of The Total Environment, 755, 142526.
834 https://doi.org/10.1016/j.scitotenv.2020.142526

835 Yang, J., Wen, Y., Wang, Y., Zhang, S., Pinto, J.P., Pennington, E.A., Wang, Z., Wu,
836 Y., Sander, S.P., Jiang, J.H., Hao, J., Yung, Y.L. & Seinfeld, J.H. (2021).
837 From COVID-19 to future electrification: Assessing traffic impacts on air
838 quality by a machine-learning model, Proceedings of the National Academy of
839 Sciences, vol. 118, no. 26. https://doi.org/10.1073/pnas.2102705118

840 Zangari, S., Hill, D. T., Charette, A. T., & Mirowsky, J. E. (2020). Air quality
841 changes in New York City during the COVID-19 pandemic. Science of The
842 Total Environment, 742, 140496.
843 https://doi.org/10.1016/j.scitotenv.2020.140496

844 Zhu, R., Anselin, L., Batty, M., Kwan, M.-P., Chen, M., Luo, W., Cheng, T., Lim, C.
845 K., Santi, P., Cheng, C., Gu, Q., Wong, M. S., Zhang, K., Lü, G., & Ratti, C.
846 (2022). The effects of different travel modes and travel destinations on
847 COVID-19 transmission in global cities. Science Bulletin, 67(6), 588–592.
848 https://doi.org/10.1016/j.scib.2021.11.023

849 Zhu, Y., Mao, L., and Zhang., X. (2020). Air Pollution and Mobility in Singapore
850 during COVID - 19 Pandemic, Technical Working Paper #04-2020, Asia
851 Competitiveness Institute Technical Working Paper Series.

852 **Appendix**

853 Appendix A: Distribution and Temporal Variation of Facebook movement and NO_2 in Indonesia, between Apr 2020 and Feb 2022.

854

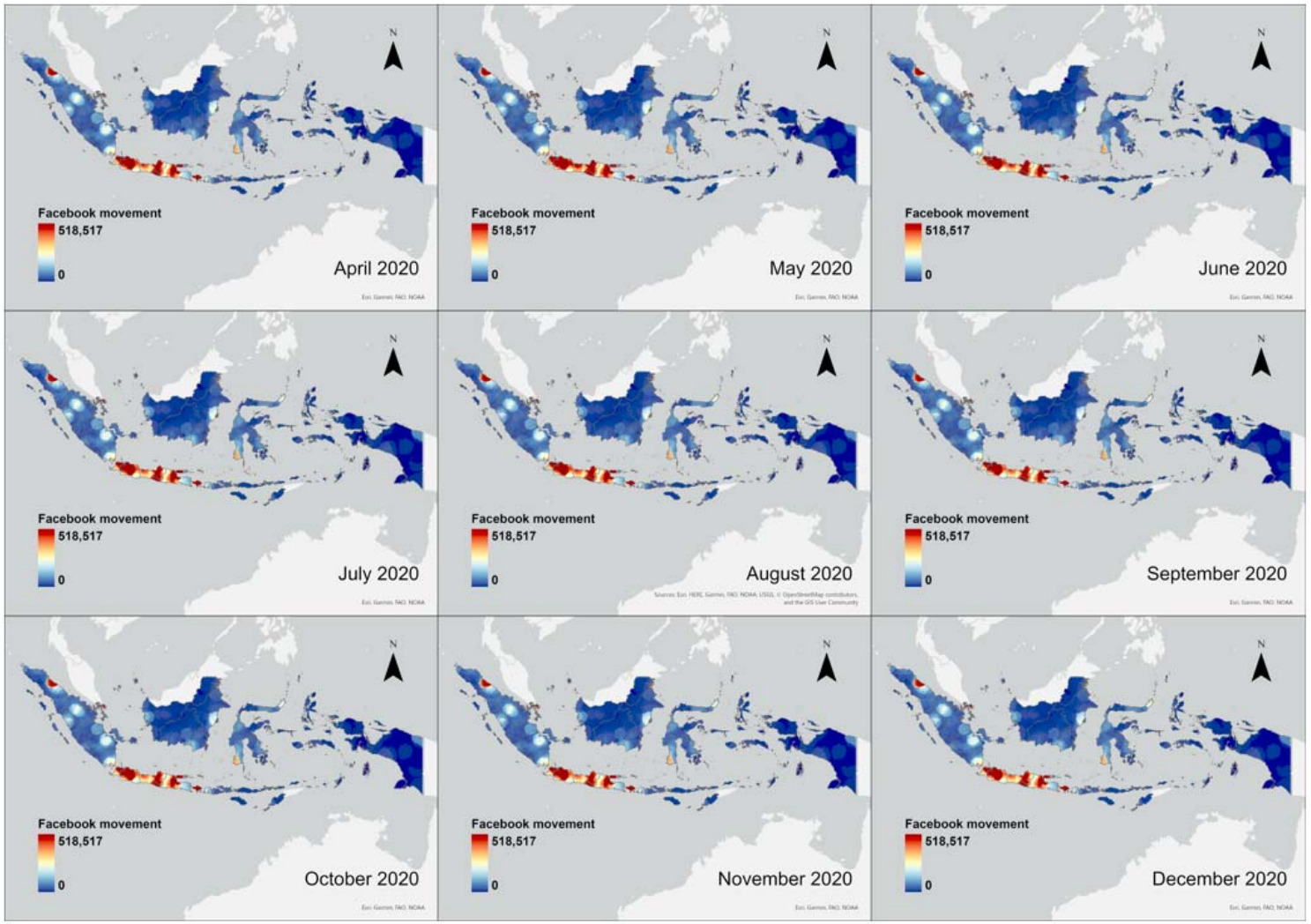

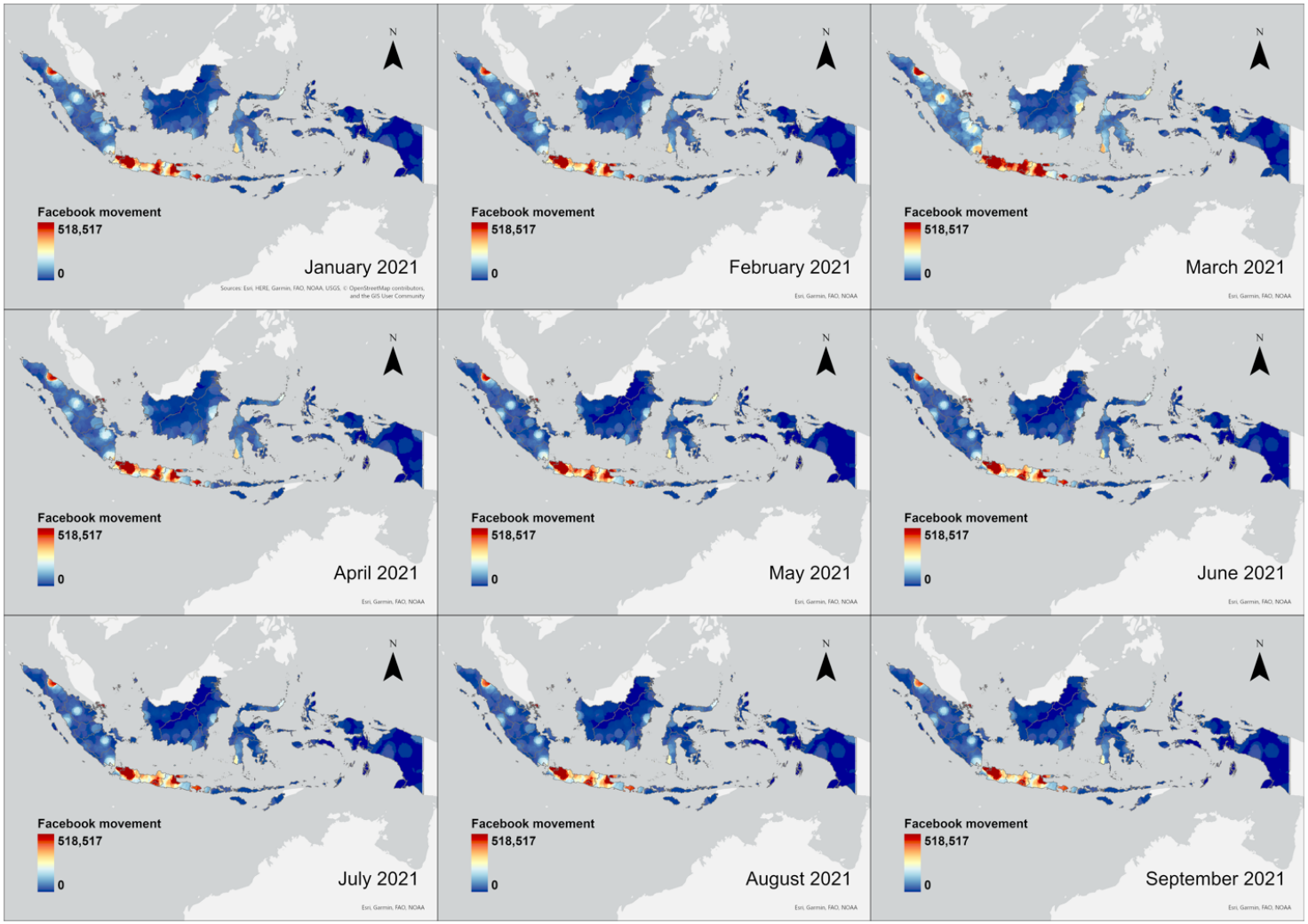

855

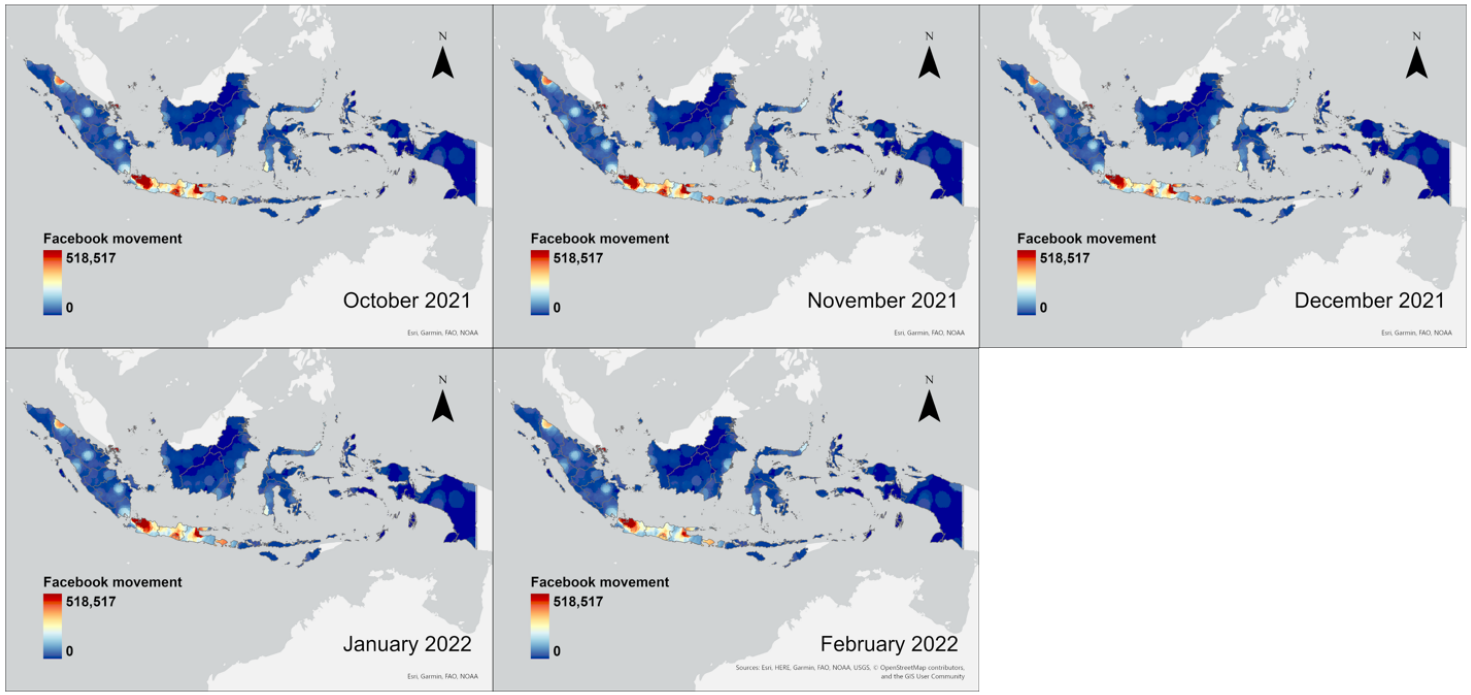

856

857

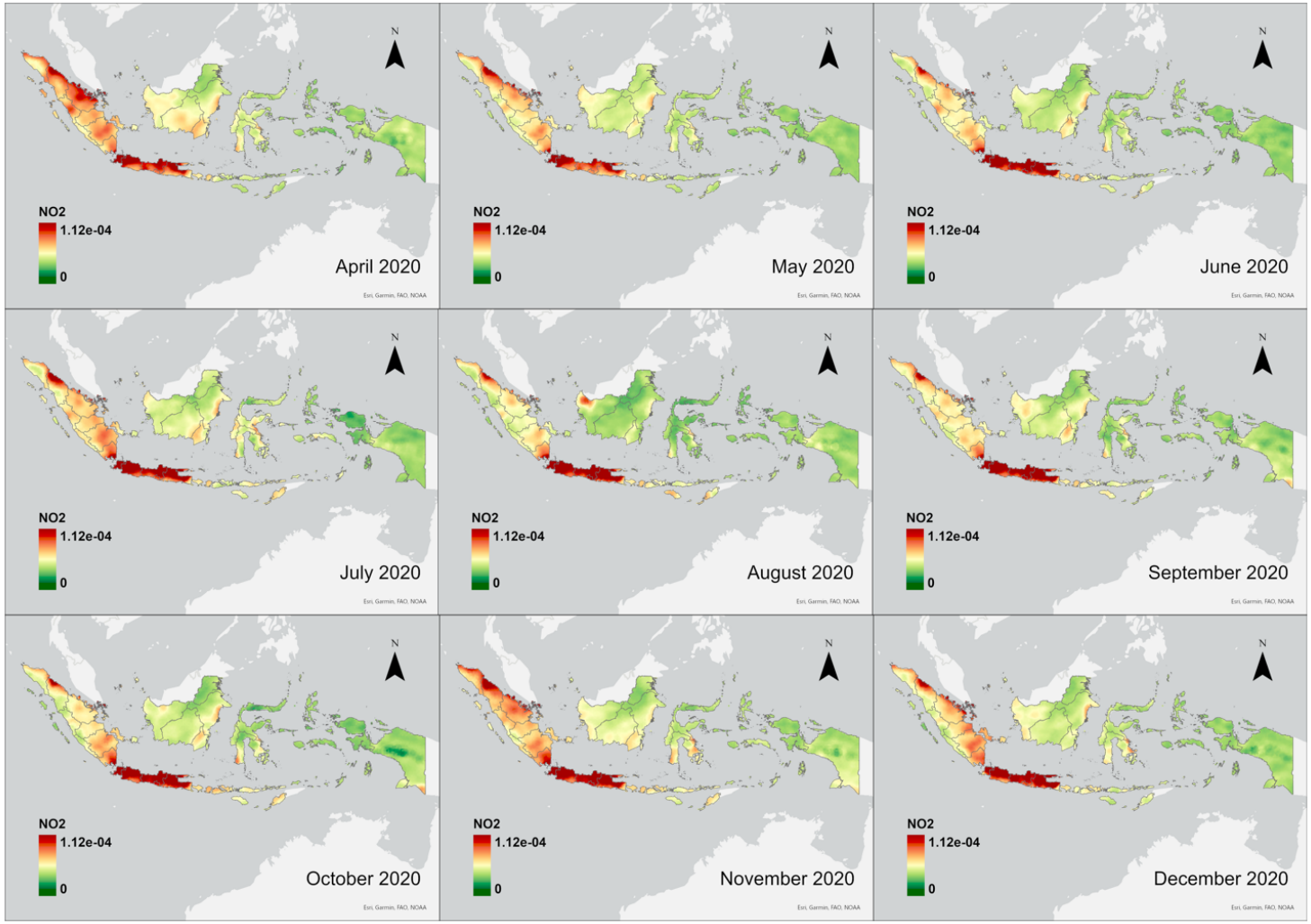

858

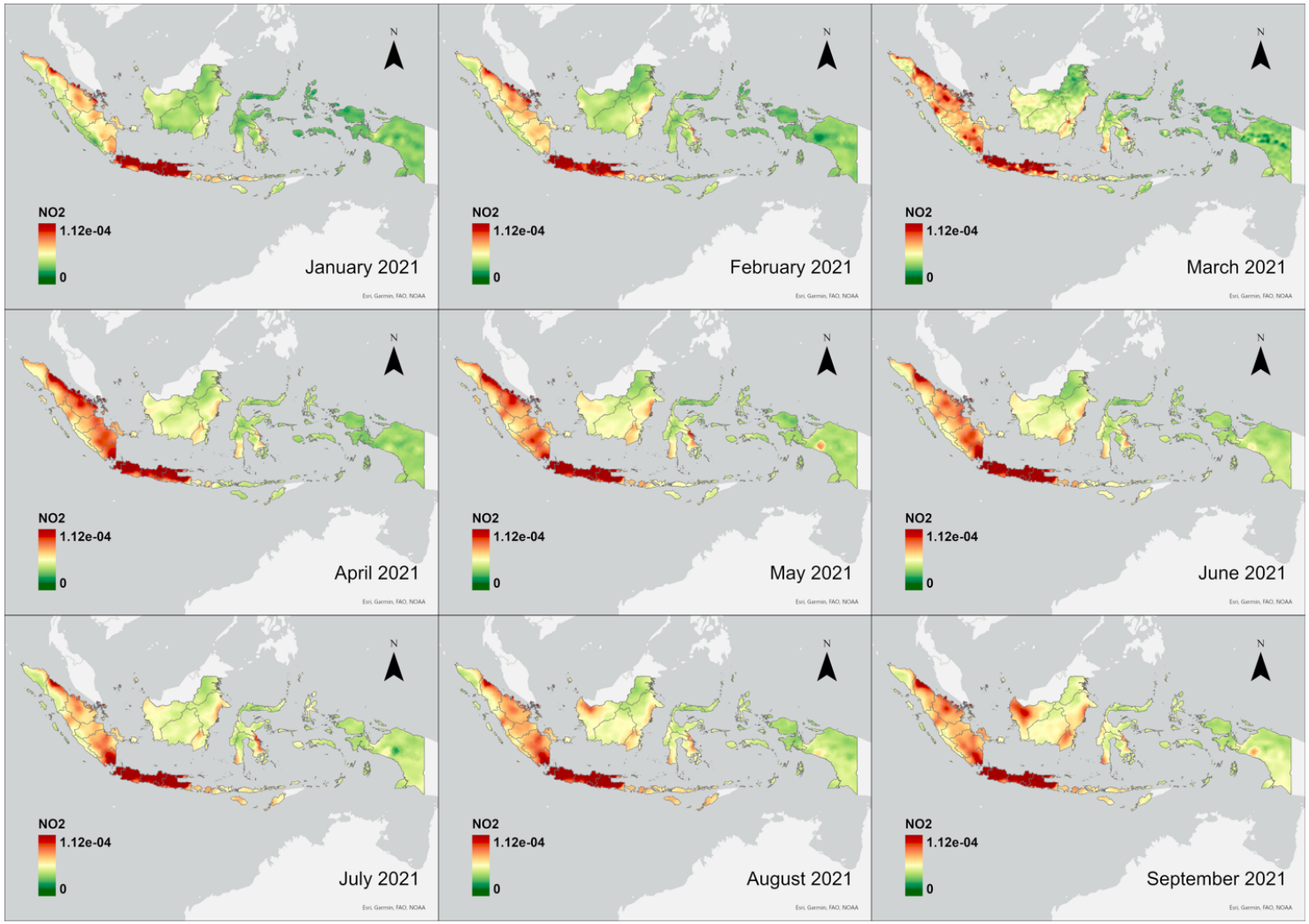

859

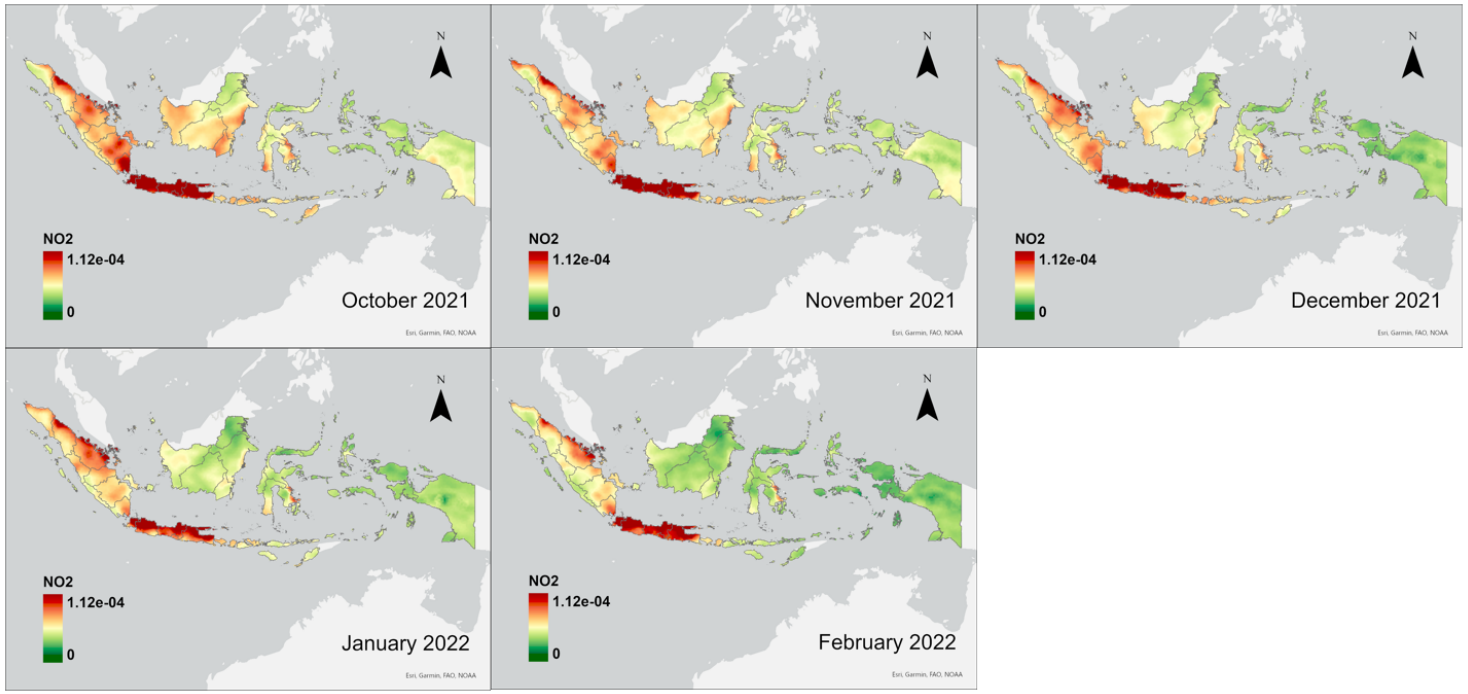

860

861